LIGAND DESIGN FOR NOVEL METAL-ORGANIC POLYHEDRA AND METAL-ORGANIC FRAMEWORKS FOR ALTERNATIVE ENERGY APPLICATIONS

A Thesis

by

RYAN JOHN KUPPLER

Submitted to the Office of Graduate Studies of
Texas A&M University
in partial fulfillment of the requirements for the degree of

MASTER OF SCIENCE

August 2010

Major Subject: Chemistry

LIGAND DESIGN FOR NOVEL METAL-ORGANIC POLYHEDRA AND METAL-ORGANIC FRAMEWORKS FOR ALTERNATIVE ENERGY APPLICATIONS

A Thesis

by

RYAN JOHN KUPPLER

Submitted to the Office of Graduate Studies of
Texas A&M University
in partial fulfillment of the requirements for the degree of

MASTER OF SCIENCE

Approved by:

Chair of Committee,	Hong-Cai Zhou
Committee Members,	Kim Dunbar
	François Gabbaï
	Hae-Kwon Jeong
Head of Department,	David Russell

August 2010

Major Subject: Chemistry

ABSTRACT

Ligand Design for Novel Metal-Organic Polyhedra and Metal-Organic Frameworks for Alternative Energy Applications. (August 2010)

Ryan John Kuppler, B.A., Miami University

Chair of Advisory Committee: Dr. Hong-Cai Zhou

The primary goal of this research concerns the synthesis of organic ligands in an effort to create metal-organic porous materials for the storage of gas molecules for alternative energy applications as well as other applications such as catalysis, molecular sensing, selective gas adsorption and separation. Initially, the focus of this work was on the synthesis of metal-organic polyhedra, yet the research has to date not progressed past the synthesis of ligands and the theoretical polyhedron that may form. Further efforts to obtain polyhedra from these ligands need to be explored.

Concurrently, the search for a metal-organic framework that hopefully breaks the record for methane adsorption at low pressure and standard temperature was undertaken. A framework, PCN-80, was synthesized based off a newly synthesized extended bianthracene derivative, yet was unstable to the atmosphere. Hydrogen and methane adsorption capacities have been evaluated by molecular simulations; these adsorption isotherms indicated a gravimetric hydrogen uptake of 9.59 weight percent and a volumetric uptake of methane of 78.47 g/L.

Following the synthesis of PCN-80, a comparison study involving the effect of the stepwise growth of the number of aromatic rings in the ligand of a MOF was pursued; the number of aromatic rings in the ligand was varied from one to eight while still maintaining a linear, ditopic moiety. The synthesis of another bianthracene-based ligand was used to complete the series of ligands and PCN-81, a two-dimensional framework with no noticeable porosity as evident by the simulated hydrogen uptake of 0.68 weight percent, was synthesized. All of these MOFs were synthesized from zinc salts to reduce the number of variables. No clear relationship was established in terms of the number of aromatic rings present in the ligand and the hydrogen adsorption capacity. However, it was confirmed that the density and hydrogen uptake in weight percent are inversely proportional. Further work needs to be done to determine what advantages are offered by these novel frameworks containing extended bianthracene derivatives. For example, with the highly fluorescent nature of the ligands from which they are composed, both PCN-80 and PCN-81 should be studied for the potential use in the application of fluorescent materials.

DEDICATION

To my family: Aubrey and McCoy

Every day with you is a blessing. I love you.

ACKNOWLEDGEMENTS

The thesis guidelines permit me to write four pages. I intend to fulfill their allotment.

I would like to first and foremost thank my advisor and friend, who has guided me in both academics and life, Hong-Cai "Joe" Zhou. Joe has always seen more in me than I have in myself. From the glory days at Miami University to the big-leagues at Texas A&M, Joe has always been there for me when I needed him. Although our work relationship has been unfairly and untimely cut short, I have no doubt our communication and friendship will endure. Thank you.

I thank my committee. You have impacted my career and will not be forgotten. François, Kim, and Dr. Jeong, thank you.

A big thanks to my post-docs and fellow researchers. I could not have accomplished what I did without you. I would like to specifically thank Dan Zhao, Andrey Yakovenko, Trevor Makal, Julian Sculley, Jinhee Park, Daqiang Yuan, Wendy Zhuang, and Luke Lu. Without your thoughtful discussion and guidance my results would not be what they are.

I would like to thank my fellow colleagues at TAMU. Specifically, Thomas Kaiser, Casey Wade, Heather Southerland, Kevin Gagnon, Houston Perry, and last but certainly not least, Chris Dorsey. In fact, I would like to especially thank Dorsey for reminding me to "quit being a woman." Although I do not share his misogynistic views, he is the only man to ever win the Daytona 500 without making a left-hand turn and is the only person I know that can sweat his own anhydrous solvents.

Without the help of TAMU's administrators, nothing would get done. Period. I would like to thank Sandy Manning and Lea Melancon for all of their help. Going out of their way to help me may have not been part of their job description, but their help and friendship have proven invaluable.

I suppose now is as good as time as any to thank the doctors who saved my life. A massive thank you to Dr. Singh, Dr. Imperial, Dr. McCoy, Dr. Lemos, Uncle Keith, Dr. Wright, Dr. Tripathy, Dr. Paull, Dr. Ortiz, all of the pathologists who analyzed said node, the oncologists at M.D. Anderson and University of Pittsburgh Medical Center, Tim Ward, and all of the nurses who cared for me. I'll keep this dedication of gratefulness to a minimum to eliminate the morbid tone.

I would like to thank any student who has the gall to trudge through this thesis. Although a thesis is supposed to be the culmination of a student's work, I feel as if this contains the tip of the iceberg of what my results could have been. Therefore, I humbly ask, and thank you in advance, that you take these preliminary ideas and run with them. I believe there is some real potential in these projects, specifically with regards to hydrogen storage. I selflessly hand them over to you. Feel free to contact me if you have questions on the direction this was heading or to discuss your ideas.

The following teachers and individuals have influenced my life over the years and I wish to thank them for that. In no discernible order: Ed Wajda, Tom Pavlansky, Maureen Bucko, Cathy Howard, Barb Graeser, Leon Ames, Chris Makaroff, Betty Ooro, Tracy Mattox, Shengqian Ma, Xi-Sen Wang, Sean Ruane, Jerry Sarquis, Lisa Perez, James Batteas, Michael Hall, and John Grunwell.

A special thanks to those few individuals who exemplified the patience, knowledge, and understanding to help me become the chemist and teacher that I am today: Tom Scott, Jian-Rong “Jeff” Li, Dave Collins, and Daren Timmons.

I would like to thank whoever isolated duloxetine and discovered its ability to block the preferential binding of norepinephrine and serotonin. I would also like to thank anyone who has donated blood or plasma. If you haven’t, please consider donating.

I would like to thank Revs. Matt Idom and Jeff Gage as well as the congregation at First United Methodist Church in Bryan, Texas. When the proverbial matter hit the fan, I know that God led us to that church. Their teachings of love, compassion, and mercy are truly inspirational and have helped guide me down the path my life was meant to take. It is only when you stop worrying about what is going to happen and put your life in God’s hands that the picture becomes clear. If ever given the chance to learn about our Father who loves us so much that He gave His Son so that we sinners may be forgiven, please take a moment to consider your faith.

The crew at Mad Hatters have poured me many a pint of Guinness over the two or so years I have been in College Station. I would like to thank not only them, but Arthur Guinness for having the vision and foresight to add a little spoiled beer to his stout. Man, I love a good Guinness.

While on the subject of fermented beverages, I would like to thank Charlie Papazian as well as the community of homebrewers on homebrewtalk.com for their guidance, advice, and insight on the finer aspects of homebrewing. All-grain brewing truly is the way to go. Remember, always indulge responsibly.

In this stream of consciousness style writing, I nearly forgot to thank my family. I thank my parents, Susan and Karl, along with Sylvia, for their exhausting support and encouragement. I also would like to thank my Grandpa for being the only person in the family who knew what I was talking about when someone inevitably would ask what my research was about.

While I am at it, I might as well thank a few friends who didn't necessarily contribute in any way, but might have listened to me gripe or offered some advice. Mike Monfredi, Rob Lee, John Heffernan, Colin Boyle, Brian Murphy, and Mike Simpson, J.D. all are good men and deserve an acknowledgement in a scholarly publication, and John says "what's up."

To anyone who has made it this far in the acknowledgements, congratulations. You may have the fortitude to tackle this entire thesis. While I am somewhat bitter about not completing my goal (yes I consider this thesis the culmination of an endeavor which I failed to complete), I am happy and content about the new direction my life has taken. I offer this advice: slow down and realize what is important in life. Your plan is not God's plan. Trust in him, love your neighbor, and accept Christ into your life. I feel blessed every day, and I hope that you will share my comfort.

Last but certainly not least, I wish to thank Dick Wolf for creating the Law and Order franchise that has become a staple in my life. Sam Watterson, if you are reading this, we named our dog after your character; that is how much you have impacted our lives. My two cents: Brisco and Green might be the best detective team ever.

TABLE OF CONTENTS

LIST OF FIGURES

LIST OF TABLES

CHAPTER I

INTRODUCTION AND RESEARCH OBJECTIVES

1.1 Porous materials

The continual search for materials to satisfy the growing needs of industry is one of the driving forces of scientific research. Among those of interest in today's cost-conscious research are materials that may be synthesized cheaply, efficiently, and effectively. Porous materials, which may be utilized for a plethora of applications, are among these types of materials. Porous materials have been used for adsorption-based gas separation and storage, shape/size-selective catalysis, drug storage and delivery, and as templates in the preparation of low-dimensional materials.[1]

Aside from possessing accessible pores, the size, shape, and volume of the pores are the most important factors in determining how well a material will perform its desired function. Table 1. shows the four IUPAC classifications based on the size of the pores for gas adsorption.[2] Adsorption isotherms are used to determine which size classification a material falls into as certain pore sizes generate distinct isotherms. There are six major isotherm types, as shown in Figure 1.

This thesis follows the style and format of *Journal of the American Chemical Society.*

Table 1. Classification of pore sizes.

Type of Pore	Pore Range in Å
Ultramicroporous	< 5
Microporous	5 – 20
Mesoporous	20 - 500
Macroporous	> 500

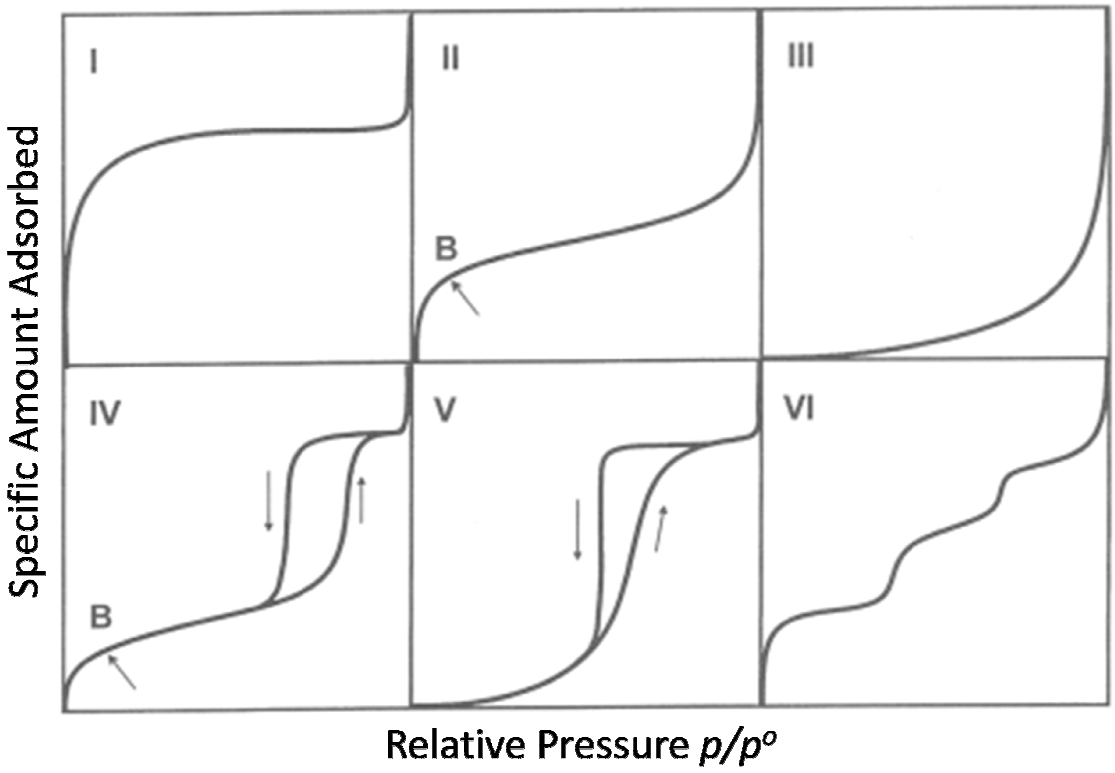

Figure 1. The six adsorption isotherm types.[3]

A material displaying Type I behavior is classified as either ultramicroporous or microporous. The Type I behavior is a result of the potential fields from neighboring walls overlapping thus enhancing the interaction energy of the solid framework with a gas molecule; at low pressures, this enhancement distorts the isotherm in the direction of increased adsorption.[4] Complete filling of the pores is therefore possible at relatively low pressures, and a plateau effect is seen when saturation has occurred.

Type II isotherms are indicative of a nonporous solid with a monolayer adsorption. Type III and VI isotherms may indicate a nonporous solid yet can also indicate a macroporous solid. The type VI appears whenever multilayer adsorption occurs as can be seen by the stepwise adsorption curve. For nonporous solids, whether a type II or III isotherm appears is dependent upon attractive interaction strengths: stronger fluid-solid attractive interactions result in a type II isotherm while stronger fluid-fluid attractive interactions result in a type III isotherm.[5] Type IV and V isotherms typically indicate a mesoporous solid although type V isotherms may also denote a microporous solid.[4] These isotherms display a unique hysteresis loop as a result of the amount adsorbed on the solid always being greater at any relative pressure along the desorption curve than the adsorption curve.[4] For a mesoporous solid, whether type IV or V isotherm behavior is displayed is once again dependant on attractive interaction strengths. Stronger fluid-solid attractive interactions result in a type IV isotherm while stronger fluid-fluid interactions lead to type V behavior.[5]

1.1.1 Carbon porous materials

In the past the search for porous materials has existed virtually exclusively in either the carbon-based or inorganic realm of chemistry. Pyrolysis of carbon-rich materials leads to the formation of perhaps the most well-known carbon porous compound: activated carbon.[6] Due to their high surface areas and porous nature, activated carbons have been used as adsorbents throughout time by a wide array of industries ranging from medicinal to military.[7] While activated carbon has the benefit of possessing high surface areas and adsorption capacities, their graphene structures suffer from a lack of order. This inconsistency prevents activated carbons from being used as materials for applications in catalysis. In fact, the distribution of the pores in activated carbons may range as widely as 20 Å to several thousand Å.[8] However, despite their lack of order, activated carbons have been a useful material for applications in gas adsorption and separation, solvent removal and recovery, and water purification for many years.

1.1.2 Zeolites

Lying in the inorganic realm of porous materials, zeolites possess the highly ordered structures that activated carbons lack. Possessing pore sizes most commonly in the range of 3 to 10 Å, zeolites are crystalline, hydrated aluminosilicates of alkali or alkaline earth metals formed from sharing the oxygen of the infinitely extending AlO_4 and SiO_4 tetrahedral frameworks.[8] Thus, zeolites may be represented by the crystallographic unit cell $M^{n+}_{x/n}[(AlO_2)_x(SiO_2)_y]^{x-} \cdot wH_2O$ where M is the metal cation of valence n and w is the number of water molecules present in the framework.[9] Elimination of the water

molecules result in the porous structures of interest. Despite this ordered porosity, zeolites are hindered in their lack of diversity, as their structures rarely deviate from Al and Si backbones.

Although there are over 40 types of naturally occurring zeolites, synthetic zeolites offer the benefit of control and purity. However, synthesized zeolites often suffer from a lack of stability as a result of the strong interactions formed between the inorganic framework and the organic template used in the synthesis. Consequently, the cationic skeleton of the framework often collapses upon removal of the template as a result of the electrostatic host-guest interactions.[10] However, the ordered structures of zeolites has enabled them to be used successfully as materials in ion exchange, separation, and catalysis for many years.[11]

1.2 Metal-organic frameworks

In an effort to combine both the high surface area and adsorption capacity of carbon-based materials with the highly ordered network of inorganic materials, coordination polymers have dramatically exploded into the forefront of porous materials research. In the most elementary sense, robust and porous coordination polymers, most commonly referred to as metal-organic frameworks (MOFs), are composed of metal ions or clusters connected by polytopic organic linkers via strong coordination bonds. Coordination polymers may form in zero, one, two, and three dimensional infinite networks.[5,12] A zero-dimensional network, otherwise known as a metal-organic ring, cage, or capsule, and in geometric terms as a metal-organic polyhedron (MOP), exists as a discrete

molecule, a one-dimensional network as a chain, a two-dimensional network is composed of layers, and a three-dimensional network consists of intersecting channels.[5,13] Each of the multi-dimensional networks may possess windows, channels, or pores with dimensions ranging from 2 to 47 Å.[14] It are these voids within the network that have attracted researchers to study the applications of these networks in the fields of gas storage,[15-17] gas separation,[18] size-, shape-, and enantio-selective catalysis,[19,20] luminescence,[21] and drug storage and delivery.[22]

In the past several decades MOFs have emerged as one of the most-researched topics in the field of coordination and materials chemistry (Figure 2). Indeed, the possibility of using MOFs as materials for virtually any application involving porous compounds makes them quite an attractive research topic. At this juncture it is necessary to indicate that although in the literature MOFs go by a variety of names (porous coordination networks, porous coordination polymers, metal-organic materials, etc.) all refer to similar if not the same types of compounds. The difference in nomenclature merely reflects the individual researchers and the type of framework. To alleviate confusion, all such materials in this thesis will heretofore be referred to as MOFs.

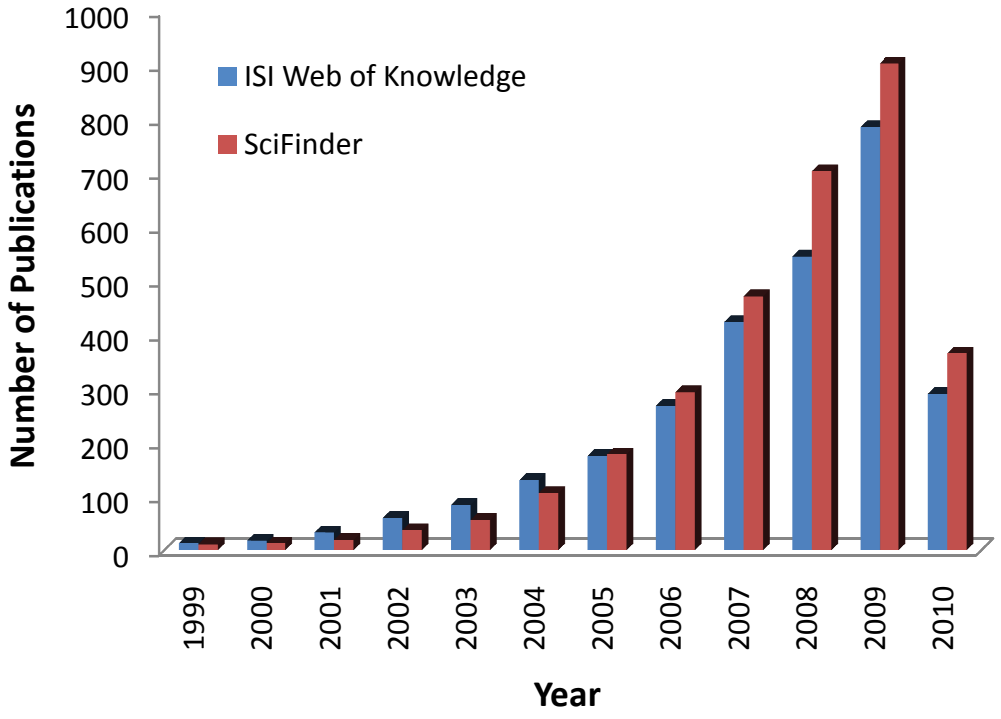

Figure 2. Number of papers on the topic "metal-organic frameworks" published from 1999 – May 2010.

1.2.1 Choice of ligand

In terms of the ligand contributing to the framework, the first consideration is usually the shape and size of the ligand. For example, ditopic ligands with bend-angles less than 180° will have a propensity to form various molecular architectures instead of three-dimensional frameworks.[13,23] Additionally, the length of the ligand will most often directly affect the size of the void space created. This is not always the case as too large

of an opening will often result in interpenetration of the framework within itself.[24,25] All of the ligands that will be discussed in this thesis are carboxylates.

A common misconception exists within the nomenclature: the ambiguity of what the ligand is. What is isolated during the organic synthesis phase of MOF construction is actually the ligand precursor, which in this case is the carboxylic acid. The ligand is the deprotonated form that actually joins the metal nodes together; carboxylates that are formed in situ from deprotonation during the solvothermal reaction are the ligands of the MOF.

1.2.2 Choice of metal

It is helpful to discuss some features of the metal centers before discussing the effect they have on the framework. A concept known as the secondary building unit has been introduced to help define the geometry adopted around the metal entities of the MOF. A secondary building unit (SBU) is the unit of "polynuclear clusters constructed from two or more metal ions and multidentate carboxylate (or other coordination moieties) linkers."[5] The SBU is unique in the sense that it is more or less a conceptual idea; the unit is usually not a reagent in the synthetic scheme but is generated in situ. Several excellent reviews have been published on the topic.[26-28] The important thing to remember is that the SBU is the initial bonding that occurs between the ligand and the metal ions. It is from the SBU that the ligands extend out in the ordered geometric array that forms the framework.

Traditionally, transition metal ions serve as the metal centers of the SBU due to their ability to adopt a large variety of coordination numbers resulting in a variety of geometries: linear, T- or Y-shaped, tetrahedral, square-planar, square-pyramidal, trigonal-bipyramidal, octahedral, trigonal-prismatic, and pentagonal-bipyramidal, as well as the distorted forms of each.[5,10,29,30] The metal that is employed in the reaction will most often dictate what SBU will form as certain metals will traditionally adopt certain geometries such as the square planar configuration with platinum. First-row transition metals are most commonly employed as the metal ions of MOFs due to their availability, cost, fixed coordination geometry, and thorough understanding of chemical bonding.[29]

Additionally, the functionality or properties of the MOF is often times directly related to the metal ion used. If one wishes to create a magnetic MOF then a paramagnetic metal ion should be incorporated.[31] The nature of the metal has also been shown to have an effect on the adsorption properties of MOFs with respect to certain gases. The metal with the known catalytic function should be incorporated if the constructed MOF is to have the desired catalytic property. To optimize the intended application, the judicious choice of both ligand and metal is important.

1.2.3 Synthetic conditions

MOFs are typically synthesized by means of a solvothermal reaction where both the metal salt or cluster and organic ligand are combined and heated at relatively low temperatures (less than 300 °C) until crystal growth has completed. The solvent employed is most often polar and possesses a high boiling point such as water, dialkyl

formamides, dimethyl sulfoxide, and dimethylacetamide. Primary concerns when synthesizing MOFs include the judicious choice of solvent, the ratio of the ligand to metal, the pH of the solution, and the solubility of the organic ligand and metal salt employed in the reaction system.

As most MOFs are insoluble once formed, the only suitable means for structural analysis is X-ray diffraction. Although research is currently underway to find a suitable means of solving MOF structure using only X-ray powder diffraction, to date the most reliable method is single-crystal diffraction. Therefore, the primary goal of MOF synthesis is to obtain good quality crystals suitable for single-crystal X-ray diffraction.[29] In an effort to obtain said crystal, much alteration is done varying the concentration of the reagents as well as the solvent and conditions of the reaction. For example, although solvothermal reactions are capable of producing excellent quality crystals, it is often necessary to attempt other setups such as the layering of solvents and setting up diffusion reactions to allow for the slow, gradual mixing of the reactants. However, solvothermal reactions remain the predominant means of synthesis. Teflon-lined stainless steel bombs, glass vials, and pyrex tubes sealed under vacuum are used as the reaction vessels depending on the amount of MOF being synthesized.

The resultant framework is a function of not only the ligand and metal employed in the reaction, but also the conditions in terms of the solvent and acids or bases added. The solvent used should be judiciously chosen as its use is not only crucial for solubility purposes but also for stability as well as defining the characteristics of the framework, or sometimes even as a template. Typically, MOFs are synthesized from solvothermal

reactions at temperatures that range between 50 and 250 °C. Therefore, solvents with relatively high boiling points such as dialkyl formamides (DMF or DEF), dimethyl sulfoxide (DMSO), dimethyl acetamide (DMA), and water are commonly utilized. Often times the solvent is incorporated into the structure of the MOF. This may be compared to the use of a template when synthesizing a zeolite except for that the solvent itself acts as a template in MOF synthesis. Additionally, the solvent may often times be removed from the framework without resulting in a collapse of the framework structure.

Occasionally the addition of small amounts of acid or base is necessary to promote good crystal growth. This is especially the case when carboxylate ligands are employed in the reaction. As previously mentioned, deprotonation is necessary for the oxygens to form bonds to the metal centers. In some instances a carefully chosen base needs to be added to promote the deprotonation; the base, such as amines, alcohols, or pyridine, needs to be cautiously chosen to avoid competition with the ligand for the open metal site. As shown in Equation 1, the deprotonation of the carboxylic acid is reversible.

Equation 1

$$RCOOH \rightleftharpoons RCOO^- + H^+$$

If deprotonation occurs too rapidly, powdered reagents are likely to crash out of solution and single crystal formation does not proceed. By Le Chatelier's Principle, the addition of a small amount of acid (commonly in the form of fluoroboric acid) will shift the equilibrium towards the carboxylic acid, thus slowing down deprotonation and thereby providing the optimal conditions for crystal growth.

As shown above, the synthesis of high-quality crystalline MOFs is dependent upon a combination of several variables. Although experience often dictates which conditions provide the best crystals, trial-and-error methods as well high-throughput approaches are often necessary.[32,33] Yet another means of MOF synthesis is that by microwave irradiation. The obvious benefit of microwaves is a much shorter crystallization time, yet they also permit the reaction to undergo a wide array of temperatures while allowing control of face morphology and particle size distribution.[34-36] The distinct disadvantage is the size of the crystals produced as they are rarely large enough to obtain good structural data by means of X-ray single-crystal diffraction. Current methods to solve MOF structures by X-ray powder diffraction are underway.

1.2.4 Structure of metal-organic frameworks

When considering the structure of MOFs it is helpful to start with the SBU. While the organic ligand may also be considered a SBU, their structures rarely deviate during the MOF reaction. Therefore, the focus with respect to SBUs lies within the initial bonding between the metal ions and the bridging ligands. Figure 3 shows four common SBUs: Figure 3 a and b shows SBUs with a trigonal and a square planar arrangement of the metal atom arrangements, respectively. Figure 3 c features a tetrahedron of metal atoms surrounding a central oxo anion, and Figure 3 d represents a dimetal paddlewheel SBU. With all of the SBUs, the edges between the two metal ions are bridged by the coordination atoms of the ligand resulting in a controlled orientation of the linker. It should be mentioned that the preferential geometry of the SBU is dependent on not only

the configuration of the ligand and the type of metal employed in the reaction, but also the metal to ligand ratio, the solvent, the reaction conditions, and the source of counterions to balance the charge of the metal ions.[37]

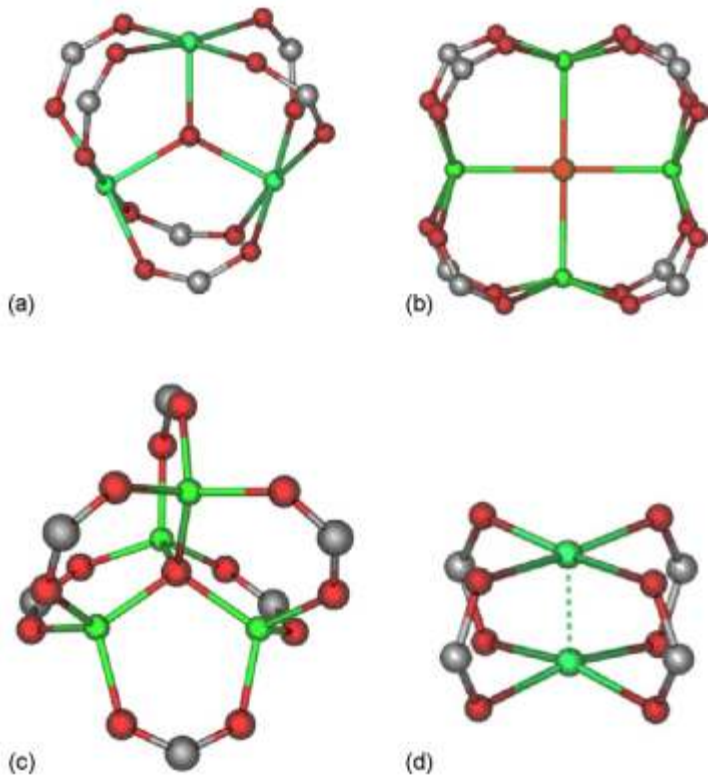

Figure 3. Structural representation of four common SBUs; green atoms are metals, red atoms are oxygen, grey atoms are carbon.

The generation of the SBU leads to the final arrangement of the linkers connecting the SBUs. The interstitial spaces created between the SBUs are the pores of the MOF. As nature abhors vacuum, guest molecules such as solvent will often times fill the void spaces formed within a MOF. Upon removal of these guests, a pore will be generated

which then enables the MOF to be used as a porous material. However, the larger the pore, the more likely is it that the framework will collapse. If the framework remains intact after guest evacuation then the MOF is said to possess permanent porosity, a highly attractive feature of MOFs.

Generally speaking, to some extent the larger the pore, the more suitable the framework is for applications in the fields of host-guest chemistry such as catalysis and as molecular carriers. Smaller pores are the result of SBUs being fixed closer together. This decreases the distance from ligand to ligand thus enabling the framework to be utilized for gas storage and separation as the guest gasses will have a strong interaction with the walls of the pore.

1.3 Metal-organic polyhedra

Metal-organic polyhedra (MOPs) are molecular cages assembled from organic linkers and metal ions or clusters (SBUs). These cages possess a well-defined geometrical structure due to the rigidity of the SBU utilized in the reaction. SBUs in this case may be either a distinct paddlewheel such as $Mo_2(CO_2)_4$ or the result of a reaction between a metal salt and a ligand in situ. Additionally, the porosity of the polyhedra are microporous in nature and has been proven to exist upon the removal of solvent molecules resulting in permanent porosity of the cage.[38] MOPs, like MOFs, are formed from supramolecular self-assembly reactions under appropriate thermodynamic conditions.[39] The inherent difference between a MOP and a MOF arises from the

discreet molecular cage of the MOP versus the infinitely extended framework of the MOF.

The assembly of a MOP is in theory much more predictable than MOF construction, a reflection of the difference between the synthesis of a molecule versus that of a framework. An intricate part of predictable synthesis is the ease in determining the final structure whether it be from powder or single crystal diffraction.[40] As a result of controlling the angle of the ditopic linker employed to connect the paddlewheel SBU, the resulting polyhedra formed from simple polygons should posses the predicted structure. A simple example is the combination of a ditopic ligand of 120° with 12 di-molybdenum paddlewheel units to form both a cubooctahedron and an anticubooctahedron depending on the ligand used and the orientation of the ligands around the paddlewheel.[41] By linking SBUs and ditopic linkers while varying the angles, multiple, predictable polyhedra may be formed to serve as building blocks for MOFs or for direct use in applications.[40,42,43]

In light of their stability, the ability of MOPs to function as SBUs for the construction of MOFs has been examined with the idea that using a MOP as the SBU will enhance the rigidity and porosity of the MOF. The MOF would then be able to retain its structure in the absence of guest/solvent molecules, thus creating a framework with permanent porosity.[44] A promising result occurred when Yaghi and coworkers were able to create a MOP of permenant porosity when they obtained crystals of MOP-1 constructed from $Cu_2(CO_2)_4$ paddlewheel.[44]

On the other hand, in order to prevent the lack of porosity that results when the occasional interpenetration occurs in MOF synthesis, MOPs may be used in the construction of MOFs. The porosity present in the SBU guarantees that the resulting MOF will possess a certain degree of porosity as interpenetration cannot effect the porosity of the SBU due to size exclusion and steric hindrance.[45] Furukawa et al. demonstrated that permanent porosity is able to exist alongside interpenetration in MOFs when MOPs are used as the SBUs.[43]

In addition to the robustness of MOPs, their solubility also makes them attractive SBUs for the construction of MOFs. Solvothermal synthetic procedures require that the species be soluble in the reaction solvent: when the organic ligands that are involved in MOP synthesis possess amine groups that are able to donate /accept a proton to / from the solvent, the resulting cage is soluble in common organic solvents such as DMF, DMSO, DMA, etc.

To date, there exist numerous examples of MOFs constructed with MOPs as their SBUs.[45-48] A common feature among these MOFs is that each framework possesses a high degree of stability. This can be attributed to the use of MOPs as the SBU as well as additional interactions such as π–π stacking and stable, non-reactive metal centers.[45] Additionally, ditopic ligands have been used to extend the MOP into the MOF.[23]

The findings of the early groups studying MOPs revealed that in addition to improving the rigidity and stability of MOFs, the porosity of the MOP, itself, may be useful for such applications as gas adsorption, catalysis, and chemical sensing.[41,47,49] For example, adsorption isotherms of MOP-23, synthesized by Yaghi and coworkers, demonstrated

that MOP-23 adsorbed up to 120 cm^3/g of hydrogen gas and 50 cm^3/g of carbon dioxide.[43] In addition, they showed that post-synthetic modification of MOP surfaces is possible. Likewise, Hamilton et al. showed that noncovalent exterior decoration of MOP surfaces is possible.[50] This opens the door for a wide range of modifications that may lead to new, intricate functions. For example, decorating the surface of a MOP with alternating hydrophilic and hydrophobic groups may create a novel SBU to be used for selective gas adsorption in resulting MOFs. Furthermore, the addition of a chiral group to the surface of a MOP may lead to the creation of a chiral MOP suitable for a wide array of chiral catalysis.

1.4 Research objectives

This thesis will provide both results and future directions of research conducted in the areas of metal-organic frameworks and metal-organic polyhedra synthesized in an attempt to create novel frameworks and cages suitable for a wide variety of applications, most notably hydrogen and methane adsorption. To avoid redundancy, each subsequent chapter will contain a relatively brief introduction of the strategies and properties of synthesized frameworks and molecules. Properties listed in this chapter should be considered applicable to the following chapters unless otherwise noted.

CHAPTER II

NOVEL LIGAND WITH 150° BEND-ANGLE TO CONSTRUCT A LARGE METAL-ORGANIC POLYHEDRON

2.1 Introduction

The continual need to create interesting, useful materials is one of the primary drives of chemists. Inorganic chemists are no different in this aspect as much research has gone into the development of new materials for useful applications. Metal-organic polyhedra (MOPs), falling under the realm of porous materials, represent a small facet of this research. A blending of the fields of porous materials and coordination chemistry, MOPs represent an area of research in which although the geometry and bonding has been extensively studied, the applications for which these polyhedra might lend themselves is relatively unexplored.

As previously explained, the relationship between ligand and cage size is usually proportional. In an effort to not only synthesize a geometrically novel cage, but also provide for the opportunity to explore the properties associated with a larger cage, a novel ligand precursor with a 150° bend-angle was designed to be synthesized. The anticipated polyhedra that would form as a result of the solvothermal reaction between 1H-indole-2,5-dicarboxylic acid and $Cu(NO_3)_2$ would result in a cage that should be larger than the MOPs formed from ligands with bend-angles of 120° and 90°, the more commonly used ligands to form MOPs. The syntheses of MOPs that are not of the platonic or Archimedean type are unique and interesting to study.

Should the resulting cage contain either an open metal site or an accessible organic functional group, the opportunity to utilize the MOP for catalytic purposes is available. As a MOP is a discreet porous molecule, the same catalytic principles apply to it as to other porous materials. Indeed, the use of MOPs for enantioselective catalysis has already been accomplished.[51]

2.2 Results and discussion

The ligand precursor 1H-indole-2,5-dicarboxylic acid was synthesized according to a modified literature method as shown in the synthetic scheme in Figure 4.[52] This molecule was obtained in pure form and was employed in several solvothermal reactions involving Cu(II), Zn(II), Co(II), and Mn(II) with solvents such as DMA, DEF, DMF, and DMSO. To date, no crystals suitable for single crystal X-ray diffraction have been obtained.

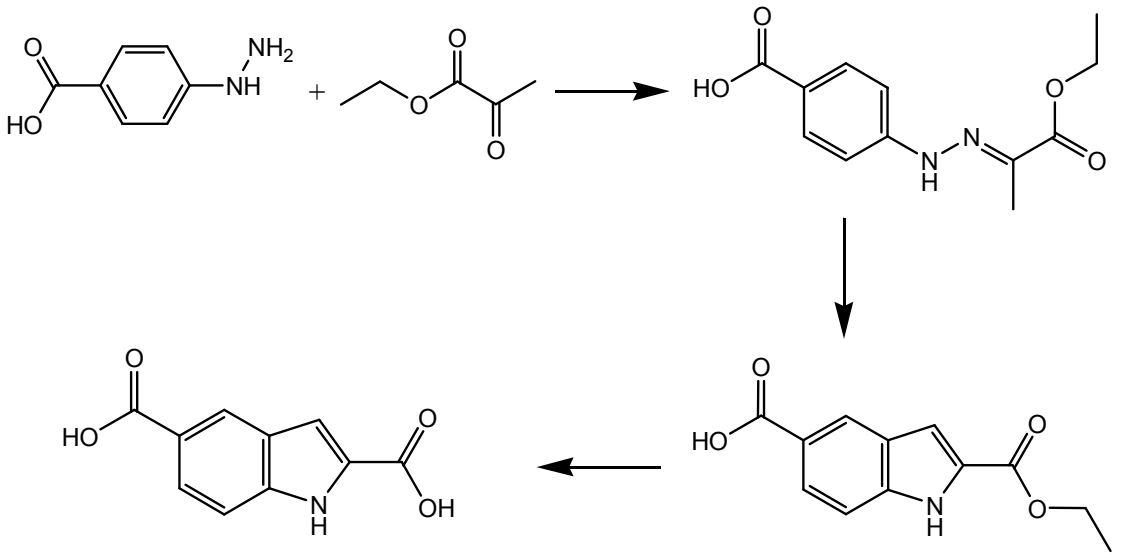

Figure 4. Synthetic Scheme for Synthesis of 150° Bend-Angle Ligand.

2.3 Future work

First and foremost, crystals from the solvothermal reaction need to be obtained. X-ray diffraction studies should reveal the structure of the polyhedra, although it is also likely that an extended MOF will be synthesized due to the large bend-angle of the ligand. Should the anticipated polyhedron be formed, the first step must be to determine if the molecule possesses an opening in which guests may be inserted and removed.

In an attempt to produce a polyhedron in which the NH group of the indole is located within the cage, the ligand precursor 1H-indole-2,6-dicarboxylic acid should be synthesized (Figure 5). Following a similar solvothermal synthesis as that which produced the previous MOP, a MOP with the NH facing toward the metal center of the MOP should be formed. Following this, a comparison should be made between the two in terms of whether or not the NH of the heterocycle facing inside or outside the cage

has an effect on the adsorption properties of the cage. Following this study, more insight will be gained in respect to the tailoring of the walls of the polyhedron to elucidate the intended application of the cage.

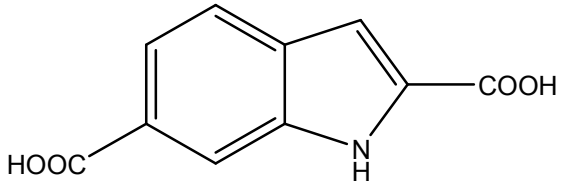

Figure 5. 1H-indole-2,6-dicarboxylic acid with 150° bend-angle.

The ability to easily modify and functionalize indoles as a result of the Fischer indole synthesis[52] makes this ligand an ideal candidate to test the effectiveness of organocatalysts that are part of the MOP.[53] Based on these results, the research can be extended one step further to determine the effectiveness of this polyhedron in terms of its ability to perform organocatalysis, for example the Knoevenagel condensation of carbon acids compounds with aldehydes to afford α,β-unsaturated compounds.[54] Secondary amines such as piperidine has been successfully proven to perform this catalytic reaction in high yields in a one-pot synthesis,[55] the addition of a piperidine to either the 4 or 7 position of 2,5 indole dicarboxylic acid will position the catalyst inside and outside the cage, respectively (Figure 6). ^{1}H NMR or HPLC could be used to quantitatively monitor the effectiveness of the organocatalysis and the effectiveness of the direction of the secondary amine could be determined. Of course, if the pore is blocked by the piperidine, then catalysis will not be able to take place. The outcome of

these reactions is going to be somewhat predetermined by the size and properties of the original polyhedron. Should the reaction proceed more efficiently with the amine facing away from the center of the cage, yet still show conversion while pointing inwards, it can be determined that the substrates do not benefit from being confined in the cage and either new substrates should be tested or a new cage created.

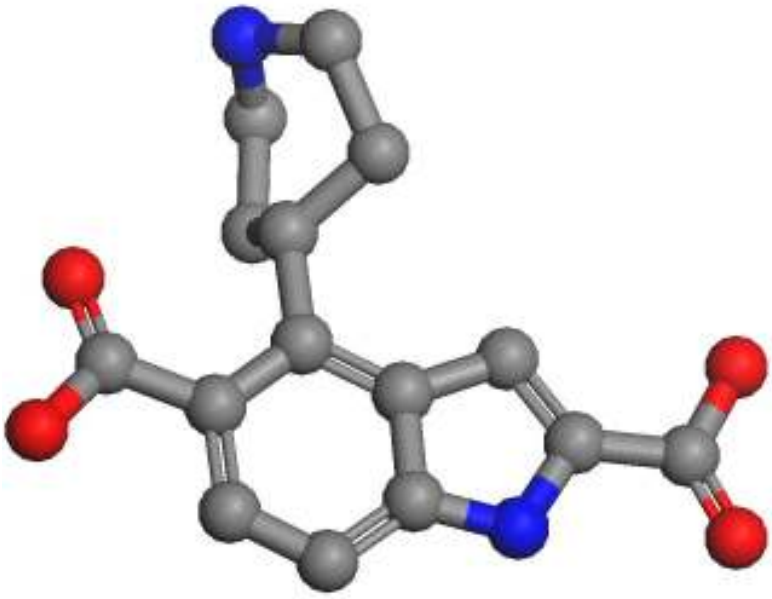

Figure 6. 4-(piperidin-4-yl)-1H-indole-2,5-dicarboxylic acid will result in a cage with the secondary amine facing towards the center of the cage, thus the catalysis will be performed inside the cage; geometrically optimized structure calculated with Materials Studio 5.0.

2.4 Synthesis

The following synthetic routes are from a modified literature procedure.[52]

Synthesis of ethyl pyruvate-4-carboxyphenylhydrazone:

4.02 g of 4-hydrazinobenzoic acid was charged in a 250 mL round bottom flask and was dissolved in a mixture of 60 mL of glacial acetic acid and 30 mL of water. The mixture was dissolved with the aid of a stirbar and heat (approximately 60° C) to form a reddish-orange solution. The flask was cooled in an ice bath and 3.05 g of ethyl pyruvate in 10 mL of glacial acetic acid was slowly added. The temperature was monitored over the addition to ensure that the solution did not rise above 10° C to produce a murky, peach colored suspension. The suspension was stirred at room temperature for one hour. The precipitate was washed with water and dried under dynamic vacuum to yield pure pale-yellow product. ^{1}H NMR (DMSO): δ 12.44 (br, 1H), δ 7.78 (d, J = 8.7Hz, 2H), δ 7.30 (d, J = 8.7 Hz, 2H), δ 4.23 (q, J = 6.7 Hz, 2H), δ 2.10 (s, 3H), 1.28 (t, J = 6.8 Hz, 3H).

Synthesis of 2-carbethoxyindole-5-carboxylic acid:

2.7 g of ethyl pyruvate-4-carboxyphenylhydrazone and 12.7 g of zinc chloride were ground in a crucible in a nitrogen glove box to form an intimate mixture. The mixture was transferred to a 100 mL round bottom Schlenk flask and cycled under nitrogen on a Schlenk line. A variac and sand-filled heating mantle were used to heat the contents of the flask above 180° C while still under nitrogen. The mixture began to darken near the base and soon formed a black solid. The septum was removed while the nitrogen was

still flowing on the line and the mixture was stirred with a glass rod. A gas was released when the mixture was stirred. When the mixture became uniformly dark, the flask was removed from the heating mantle. 35 mL of water and 1 mL of hydrochloric acid was added. A condenser was attached and the suspension was refluxed for ninety minutes. The solid was collected on a fritted filter and washed with ice-cold water. The dark, reddish brown solid was recrystallized in boiling glacial acetic acid followed by a wash with cold acetic acid. The product was then dissolved in dichloromethane and passed through celite. Pure 2-carbethoxyindole-5-carboxylic acid was collected as a dark, brownish-yellow solid. ^{1}H NMR (DMSO): 12.48 (br, 1H), 12.20 (s, 1H), 8.42 (s, 1H), 7.79 (d, J = 9.0 Hz, 1H), 7.51 (d, J = 9.0 Hz, 1H), 7.33 (s, 1H), 4.33 (q, J = 6.8 Hz, 2H), 1.36 (t, J = 4.0 Hz, 3H).

Synthesis of 2,5 indole dicarboxylic acid:

0.75 g of 2-carbethoxyindole-5-carboxylic acid and 2.7 g of sodium hydroxide were dissolved in a 100 mL round bottom flask and refluxed in 30 mL of water for four hours. Activated carbon was added to remove inorganic impurities. The mixture was then filtered and the filtrate was treated with 12.1M hydrochloric acid until precipitate appeared. The precipitate was filtered and dried overnight *in vacuo* to produce pure 2,5 indole dicarboxylic acid a dark yellowish-brown powder. ^{1}H NMR (DMSO): δ 11.31 (s, OH), δ 7.72 (s, 1H), δ 7.20 (d, J = 8.7 Hz, 1H), δ 6.86 (d, J = 9.0 Hz, 1H), δ 6.51 (s, 1H).

CHAPTER III

EXTENDED CARBAZOLE-BASED LIGAND IN EFFORTS TO SYNTHESIZE EXTENDABLE METAL-ORGANIC POLYHEDRON

3.1 Introduction

It has been recently demonstrated that the conversion from molecular polyhedra to metal-organic framework and back to molecular polyhedra is possible.[23] In this manner, the polyhedron may be viewed as a direct building block for the framework. Serving as a pseudo-SBU in the sense that the polyhedron that appears in the final framework is synthesized prior to the reaction, a linker would join the polyhedral centers to create a framework. This supramolecular assembly approach has been proposed and a design elaborated,[56] yet to date only one example of this technique has been carried out successfully.[23]

One immediate prerequisite that must be satisfied is that the building blocks must be soluble in order for the next step in the synthesis to be carried out. With traditional MOF synthesis this is usually not a problem (provided something large such as dendritic linkers are not employed) as the metal salts and organic linkers are usually quite soluble in the chosen solvents. However, with this supramolecular building block approach, the polyhedra to serve as the nodes of the framework may not always be soluble, resulting in an inability for a further reaction to a MOF.[57] Thus, a judicious choice of the organic ligand employed in the polyhedra reaction scheme is of primary concern.

It has been demonstrated in the literature that a reaction between 9H-carbazole-3,6-dicarboxylate (H_2CDC) and $Cu(NO_3)_2 \cdot 2.5\ H_2O$ in a 1:1 solution of DMA:ethanol affords blue-green crystals of $[Cu_2(CDC)_2(DMA)(EtOH)]_6 \cdot xS$ (S = noncoordinated solvent molecule) as shown in Figure 7.

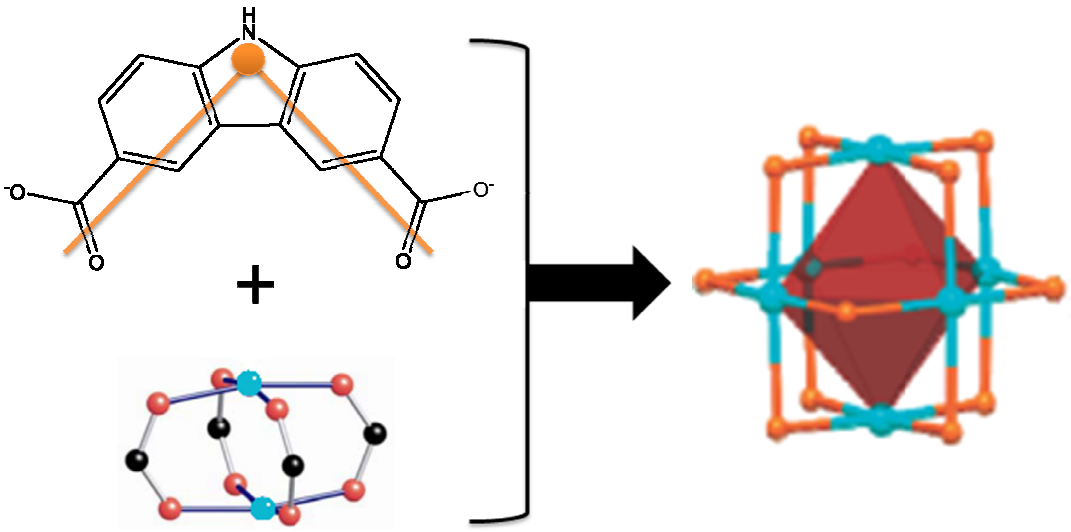

Figure 7. 90° bend-angle carbazole ligand joined with copper paddlewheel to form molecular polyhedron.[23]

The polyhedron formed in this reaction is an octahedral cage with six axial copper-paddlewheel nodes of the formula $Cu_2(CO_2)_4$ which are linked together by 12 CDC ligands. This polyhedron crystallized in an O_h symmetry when ignoring the axially coordinated solvent molecules. These crystals are stable to oxygen and have been isolated. By utilizing a linear, ditopic ligand to connect the six vertices of the octahedron, the polyhedral cage was extended into a three-dimensional framework: a solution of $[Cu_2(CDC)_2(DMA)(EtOH)]_6 \cdot xS$ dissolved in diethylformamide was layered

with a solution of excess 4,4'-bipyridine dissolved in ethanol to afford SEMOP-1 (soluble and extendable metal-organic polyhedra).[23]

3.2 Results and discussion

The significance behind this work lies in the fact that a MOF was created using a step-wise approach in which the ultimate framework was predicted before synthesis occurred. Often times, it is claimed that a MOF structure is designed to have the resultant outcome. Much disagreement exists in the field with respect to this alleged design.[10,58] However, by first constructing a polyhedron of a well-studied geometry followed by employing a simple extending ligand to connect the vertices, a rational prediction may be made and the ultimate structure realized.

In an effort to extend this work, a novel ligand-precursor with the same 90º bend-angle was synthesized: 4,4'-(9-ethyl-9H-carbazole-3,6-diyl)dibenzoic acid (H_2CDB). H_2CDB differs from H_2CDC in two ways: H_2CDB may be thought of as an extended version of H_2CDC as two aromatic rings protruding from the 4 and 7 positions of the carbazole molecule maintain the 90º bend-angle, and the H atom extending from the N atom of the carbazole is replaced by an ethyl group (Figure 8). In H_2CDC the N-H functional groups of the ligands are able to form hydrogen bonds with solvent molecules, thus improving the solubility of the resultant molecular polyhedron.[23] The longer ligand-precursor, H_2CDB, is much more insoluble than H_2CDC. As a result, the resultant MOP would not be as readily soluble as SEMOP-1. To combat this, an ethyl group was chosen in lieu of the H atom at the 9 position of the carbazole.

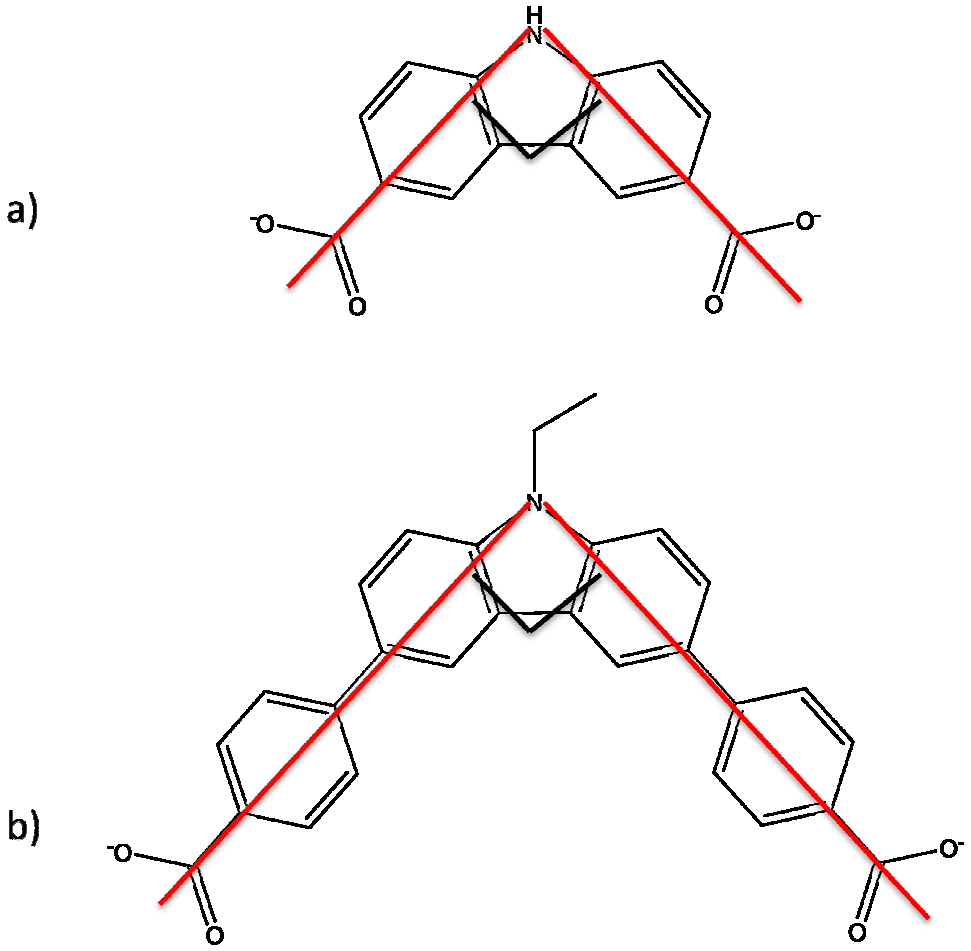

Figure 8. a) 9H-carbazole-3,6-dicarboxylate (H_2CDC) and b) 4,4'-(9-ethyl-9H-carbazole-3,6-diyl)dibenzoate (H_2CDB) both possess a 90° bend-angle.

It has been suggested that MOFs with cage-like polyhedral building units could be useful in the storage of small molecules, because adsorbed guests may remain kinetically trapped inside the cages.[59]

The ligand-precursor 4,4'-(9-ethyl-9H-carbazole-3,6-diyl)dibenzoic acid was obtained in pure form and several reaction schemes based off of the synthesis of SEMOP-1 have been employed in an attempt to obtain a crystal polyhedron. Although reactions with Zn,

Cu, Mn, and Co salts with a wide array of solvents such as DMF, DEF, DMSO, and DMA have been attempted, crystals have yet to be synthesized.

3.3 Future work

Once a high-quality crystal is obtained, the structure will be solved utilizing X-ray diffraction. Theoretically, the polyhedron will be another octahedron yet have a larger cavity than the 13.8 Å of SEMOP-1 as the extended ligand, which contains an extra benzene ring on each side of the carbazole, is longer than CDC. Each benzene, with an approximate atom to atom diameter of 2.8 Å, should extend the distance between metal centers, and thus the cavity.

Assuming an isoreticular scenario,[60,61] which is very likely upon polyhedron formation, the resulting cage should be a larger version of SEMOP-1. Should the axial positions of the paddlewheels remain uncoordinated (with respect to anything other than removable solvent), then it should follow that the extension of the polyhedron into a framework could easily be accomplished. The resultant MOF should have considerably larger pores than its predecessor. In this fashion, MOFs with not only permanent porosity but also large, accessible pores may be synthesized.

Should the resulting MOF form an interpenetrated structure, which is not unlikely considering the length of the ligand involved in the MOP formation, interesting properties may ensue as useful porosity is often exhibited in interpenetrated structures.[10,25,62,63] The reduced pore size may prove to be beneficial in the selective adsorption of gases having a small kinetic diameter.[18] It is important to keep in mind that

a reduction in pore size as a result of interpenetration does not mean that the porosity does not exist; it has merely been decreased. Any MOF constructed from a MOP will have some degree of permanent porosity as long as the polyhedra used as the SBU possesses porosity.

This unique way of ensuring porosity and preventing interpenetration provides for a much more predictable synthesis of MOFs which aides in not only the solving of the crystal structure, but also the construction of MOFs with an intended design for applications such as catalysis and gas adsorption. Most of the MOPs that are extended into MOFs in the literature are generated in situ. By synthesizing and isolating the MOP before extending it into a MOF, researchers can have more control over the structure of the framework. This will aid in the tailoring of MOFs for their intended applications.

3.4 Synthesis

3,6-dibromo-9-ethyl-9H-carbazole:

9-ethyl-9H-carbazole (2.020 g, 10.359 mmol) was charged in a 250 mL round bottom flask. 100 mL of glacial acetic acid was added and the solution stirred to dissolve the reagent. Upon dissolving, the solution turned from clear to deep purple. Bromine (1.10 mL, 21.60 mmol) was added dropwise over 20 minutes with the aid of a syringe pump resulting in a dark brown solution. The solution was poured into ice water to precipitate a white-yellow product. This was filtered and collected. The crude product was recrystallized in 100 mL ethanol to yield a pure white product. Yield: 62.92% (2.288g,

6.518 mmol) ^{1}H NMR ($CDCl_3$): 8.15 (d, J = 2.1 Hz, 2H), 7.57 (dd, J = 6.9 Hz, 1.8 Hz, 2H), 7.29 (d, J = 8.7 Hz, 2H), 4.41 (q, J = 7.2 Hz, 2H), 1.38 (t, J = 7.2 Hz, 3H).

4,4'-(9-ethyl-9H-carbazole-3,6-diyl)dimethylbenzoate:

3,6-dibromo-9-ethyl-9H-carbazole (1.585 g, 4.516 mmol), cesium fluoride (2.359 g (16.074 mmol), tetrakis(triphenylphosphine)palladium(0) (0.315 g, 0.273 mmol), and of 4-(methoxycarbonyl)phenylboronic acid (1.547 g, 8.594 mmol), and a stirbar were charged in a 250 ml Schlenk flask. A vigreux condenser was attached, and the flask was filled with nitrogen gas and evacuated on a Schlenk line three times. 200 mL of DME was degassed DME was transferred via a canula to the reaction vessel and the solution was heated to 85 °C and stirred. After seven days, the reaction was quenched with the addition of excess water. The mixture was passed through a filter and the filtrant discarded. The remaining precipitate was then washed with acetone and filtered again. The filtrant was again discarded and the precipitate was washed thoroughly with THF and filtered once more. The filtrant was collected and concentrated down under vacuum to yield pure product. Yield: 40% (0.893 g, 1.928 mmol) ^{1}H NMR (DMSO): δ 8.78 (s, 2H), δ 8.07 (d, J = 6.9 Hz, 4H), δ 7.98 (d, J = 6.9 Hz, 4H), δ 7.91 (d, J = 8.7 Hz, 2H), δ 7.75 (d, J = 8.7 Hz, 2H), δ 3.88 (s, 6H), δ 4.52 (q, J = 7.2 Hz, 2H) δ 1.35 (t, J = 3.3 Hz, 3H).

4,4'-(9-ethyl-9H-carbazole-3,6-diyl)dimethylbenzoic acid:

(175.3 mg, 0.3785 mmol) and sodium hydroxide (121 mg, 3.026 mmol) were dissolved in a 100 mL round bottom flask with 10 mL water, 10 mL methanol, and 20 mL of tetrahydrofuran. A condenser was attached and the reaction was refluxed for one day. The flask was removed from the heat and the solution was passed through filter paper. The solution was then acidified with hydrochloric acid to yield as a pure white solid. Yield: 37.64% (62 mg, 0.1425 mmol) ^{1}H NMR (DMSO): δ 12.84 (br OH) δ 8.70 (s, 2H), δ 7.98 (d, J = 8.7 Hz, 4H), δ 7.88 (d, J = 8.7 Hz, 4H) δ 7.83 (d, J = 9.0 Hz, 2H), δ 7.67 (d, J = 8.7 Hz, 2H), δ 4.44 (q, J = 9.0 Hz, 2H) δ 1.29 (t, J = 6.9 Hz, 3H).

CHAPTER IV

METAL-ORGANIC FRAMEWORK FOR HIGH HYDROGEN AND METHANE UPTAKE

4.1 Introduction

Briefly mentioned in Chapter I was the potential application of MOFs being used as adsorbents for gases; perhaps the most important of the gases are hydrogen and methane as they have potential applications as alternative energy sources. This introduction will address the necessities for these gases to be utilized in what is perhaps the most well-known alternative energy issue: alternative fuels for automobiles.

4.1.1 Hydrogen storage

Hydrogen possesses nearly three times as much gravimetric heat of combustion as gasoline (120 MJ/kg for hydrogen versus 44.5 MJ/kg for gasoline) making it a very attractive alternative energy source.[64] This means that the amount of hydrogen needed to power a traditional combustion engine 400 km (approximately 250 miles) is a mere 8 kg compared to 24 kg of gasoline.[65] Moreover, the oxidation of hydrogen, the means in which energy is generated, produces water as its only by-product. However, despite hydrogen being an excellent candidate for carrying energy, it suffers from a lack of efficient, effective, and, most importantly, safe storage.[16] These hurdles for hydrogen lie in the fact that it is very difficult to compress hydrogen for on-board storage in automobiles.

Although the gravimetric attributes of hydrogen are much more alluring than gasoline, volumetric comparisons reveal the short-comings. In its gaseous state, the 8 kg of hydrogen needed to power an automobile 400 km occupies a staggering 90 m^3 of volume at standard pressure. Additionally, to store the gaseous hydrogen in a fuel tank at ambient temperature would require a staggering 700 atm of pressure to be applied to the compressed tank.[66] Even when liquefied, hydrogen has a much smaller volumetric heat of combustion than gasoline: 8,960 MJ m^{-3} vs. 31,170 MJ m^{-3}, respectively.[65] Even neglecting the differences in volumetric combustion heats, the energy costs to liquefy the hydrogen and cool its' cryogenic tank would consume roughly 22% of the recoverable energy.[16,64] Therefore, the key to hydrogen storage lies in an effective way to store gaseous hydrogen. In order to guide the research of hydrogen storage materials, the DOE has set goals to be reached by 2010 and 2015 for viable hydrogen storage technologies. By 2010 the goal of 6 weight percent and 45 g/L for on board storage materials is to be reached. This is supposed to be increased to 9 weight percent and 81 g/L by 2015.[16] All of these benchmarks are meant to be reached within the temperature range of -30 – 50 °C.[67]

Eliminating high pressure and cryogenic tanks for safety and practicality purposes results in two options for storing hydrogen for on-board use: chemisorption and physisorption. Chemisorption occurs when a dihydrogen molecule comes into contact with the surface of a sorbent and is split into individual hydrogen atoms. These atoms may have a very strong affinity for the surface which will result in the formation of a hydride. The nature of the short bonds of the hydride may lead to a high hydrogen

adsorption capacity. However, this increased capacity comes at the expense of kinetic and thermal problems as loading times are commonly complete in no fewer than several hours, and the temperature required to release the hydrogen is commonly higher than 300 ºC.[68]

In order to increase the capacity of the sorbent with respect to chemisorption, the hydrogen spillover approach has been investigated. In order for hydrogen spillover to occur in MOFs, the MOF must first be doped with a metal such as Pt. Upon the introduction of hydrogen to the MOF, the hydrogen molecules dissociate on the doped metal and is then "spilled over" onto the MOF.[66]

Physisorption, the much more studied method of hydrogen storage in MOFs, occurs when the hydrogen interacts weakly with the sorbent (mostly through van der Waals forces) as opposed to forming chemical bonds as in chemisorption. Very low temperatures or very high pressures are needed to compensate for the lack of bond formed between the framework and the hydrogen molecule.[69] However, as doping the MOF with a metal is not required for physisorption to occur, the majority MOFs studied for hydrogen storage adhere to this method of adsorption.

Several methods have been developed to increase the hydrogen storage capacity such as increasing the surface area, reducing the pore size to approximately that of molecular hydrogen (approximately 2.8 Å), and increasing the number of aromatic rings within the ligand of the MOF. In theory, an increase in surface area allows for more hydrogen to come in contact with the MOF thereby increasing the overall storage capacity. However, studies have shown that there is no direct correlation between total hydrogen uptake and

surface area, as factors such as pore size, catenation (interpenetration) and ligand functionalization come into play.[70,71] By decreasing the pore size of the MOF, the attractive potential fields of the opposite walls overlap which thereby increases the hydrogen - MOF binding energy.[70-72] It has been suggested that a pore opening of approximately 6 Å will optimize the potential field interactions and overall van der Waals forces of the framework acting upon the hydrogen.[73] Increasing the number of aromatic rings within the MOF's ligand allows more than one hydrogen molecule to bind on each side.[71,74]

4.1.2 Methane storage

In addition to hydrogen, natural gas, which is composed of over 95% methane (with the remaining percentage composed of hydrocarbons, nitrogen, and carbon dioxide), is another contender for on-board vehicular storage. The overabundance and underutilization of natural gas makes it quite an attractive replacement for gasoline. The emission of carbon dioxide released is also less for natural gas than for gasoline (50 g CO_2/MJ vs. 69.3 g CO_2/MJ, respectively)[75] Natural gas has a slightly larger gravimetric heat of combustion than gasoline (50.0 MJ/kg vs. 44.5 MJ/kg), yet, like hydrogen, the hurdle lies in its storage.[64] In its liquid form, which requires cryogenic conditions to exist, natural gas possess only 72% of the volumetric energy density of gasoline.[76] With any cryogenic storage vessel, the pressure build-up from the boil-off of the liquid requires that a release vent exist to prevent an explosion. Obvious safety concerns are present with the cryogenic storage tanks for liquid natural gas.[76]

The cryogenic requirement is lifted when natural gas is in the compressed gaseous state at 3000 psig, yet this provides only 26% of the volumetric energy density of gasoline. However, the expensive multi-stage compressors and high-pressure meters needed require a great deal of cost and energy to operate, and the compressed tanks are bulky and take up valuable on-board cargo space.[76] Indeed, safety concerns arise whenever a substance is stored at a pressure as high as 3000 psig.

Adsorbed natural gas, on the other hand, is able to be stored effectively at a much lower pressure of 500 psig.[76] This lower pressure does not require the multi-stage compressors utilized with compressed natural gas systems meaning that the average automobile owner would be able to use a relatively inexpensive single-stage compressor to fill their tanks with natural gas at home. The maximum volumetric energy density achieved with adsorbed natural gas is approximately 20% that of gasoline.[76] Although this means that an automobile powered by adsorbed natural gas could only travel one-fifth as far as one powered by gasoline, the lower price and surplus of natural gas results in extracting more mileage per dollar spent. This, coupled with the lack of environmentally harmful emissions associated with gasoline, makes natural gas a very attractive fuel alternative.

In order to use natural gas to power automobiles, the adsorbent on which the natural gas is adsorbed needs to be able to store natural gas to the point where the volumetric energy density approaches that of gasoline. When focusing on adsorbents, the adsorbate of which is most important is methane, as that is the primary component of natural gas. Although activated carbon materials have been promoted as one of the best adsorbents

for methane, MOFs can make up for the short comings exhibited in activated carbons. The consistency of the crystalline samples of MOFs that exists from sample to sample is lacking in activated carbons. Additionally, as previously discussed, the tailoring of the reagents involved in the MOF allows for better tunability and functionality than in activated carbon.[77] For example, it is easier to synthesize a MOF that consistently has a pore diameter of approximately 8 Å, the optimal theoretical value (ignoring heat and mass transfer effects) at which each pore can accommodate two layers of methane, than an activated carbon where their pore sizes will vary from synthesis to synthesis.[78]

Like hydrogen adsorption, methane adsorption in MOFs is a process generally governed by physisorption. In order to achieve the highest methane adsorption per mass or volume unit, the MOF should possess a largely accessible surface area, a high free pore volume, low framework density, and a strong interaction with the adsorbed methane molecules which can be measured by the isosteric heat of adsorption at low loadings.[77,79] However, these properties often are inversely related to one another creating problems for MOF researchers. For example, an increase in the free volume of a pore will most certainly expand the opening of that pore thereby reducing the strength of the interaction with the methane and the pore wall.[77]

However, unlike hydrogen, the 20 kJ/mol heat of adsorption for methane is already in the scope of practical usage.[1] In an effort to guide the research, the Department of Energy (DOE) has set a storage goal of 180 v/v at ambient temperature and pressures not to exceed 35 bar by the end of 2010.[80] In terms of energy density, this volumetric capacity is equivalent to the amount of methane compressed at 250 bar.[81] Although

several carbon materials have surpassed this target, their limited packing density prohibits them from becoming viable materials for onboard methane storage. Additionally, it is very difficult to increase the surface areas of these materials as they appear to have nearly reached their maxima at approximately 3500 m^2/g.[81] In 2008, the Zhou lab exceeded this DOE goal with the microporous MOF PCN-14. With an absolute methane-adsorption capacity of 230 v/v at room temperature and 35 bar, this MOF exceeds the DOE goal by 28%.[82]

Knowing where the methane is stored in PCN-14 enables researchers to design MOFs more suited for methane adsorption. Grand canonical Monte Carlo (GCMC) simulations performed on PCN-14 indicated that the primary adsorption site for methane was the open metal sites of the $Cu_2(CO_2)_4$ paddlewheel.[83] This is a result of the strong binding energy associated with the Coulombic attraction between the open metal site and the slightly polarized methane molecules.[84] Although methane is a highly-symmetrical, nonpolar molecule, the unscreened interaction between the open metal ion and the methane molecule disturbs the charge distribution of the methane thereby breaking the T_d symmetry resulting in multiple moments.[84] It is this Coulomb attraction that is responsible for the extremely high initial isosteric heat of adsorption of 30.0 kJ/mol.[84]

Although the primary adsorption site for methane is the open metal position of the dicopper paddlewheel, there exist other adsorption sites throughout the framework. A good deal of methane is located within the narrow, small cages created by the anthracene chains.[83] Contributing to this attraction is the good geometrical matching of the tetrahedral methane and the deep potential pocket of the small cages which allows the

methane molecules to fit in perfectly.[83] This results in an increase in the van der Waals forces which allows for a great deal of methane to be accommodated in the cage. As shown previously, methane molecules have preferential occupancy to smaller pores which can be attributed to the stronger confinement effects and dispersive and electrostatic interactions.[85] The increase in van der Waals interactions, coupled with the Coulomb attraction of the open metal site, is what accounts for the strong adsorption sites and high uptake found in PCN-14.

4.1.3 Molecular simulations

Ideally, experimental isotherms and sorption experiments are performed to gain information on the properties of synthesized MOFs, such as surface area, pore volume, and gas adsorption capacity. However, when such experiments are unable to be performed, molecular simulations can give researchers a great deal of insight as to the potential applications for which a material might be useful. Of course, without real laboratory experimental data, simulations are only an indication of the possible properties of a MOF.

All molecular simulations performed on the discussed MOFs were carried out using Metropolis GCMC simulations on Materials Studio 5.0 to simulate a rigid framework as opposed to a flexible one. Additionally, the simulations are calculated at a fixed volume, temperature, and chemical potential while varying the pressure from 0 – 101.33 kPa (1 atm) for low pressure studies and 0 – 10000 kPa (100 bar). The GCMC simulation is

performed by randomly inserting, deleting, and rotating millions of sorbate molecules that are either accepted or rejected based on Boltzmann weighting.[86]

Whenever a comparison is to be drawn between experimental and simulated adsorption data, the following needs to be understood: simulated isotherms in Materials Studio are reported in absolute adsorption (the total number of molecules present in a framework) whereas experimental data is commonly reported in excess amount adsorbed (the number of molecules adsorbed on the surface of a sorbent). These two amounts can be related to one another following Equation 2 where N_{abs} is the absolute adsorption, N_{ex} is the excess adsorption, p is the bulk density of the sorbate, and V_{pore} is the pore volume of the sorbent.[16,86]

Equation 2.

$$N_{abs} = N_{ex} + pV_{pore}$$

With that in mind, the comparison between simulated and experimental isotherms have has been in good agreement in several reviews.[86,87] However, there have been instances in which the simulated data has overestimated the quantity of adsorbent as a result of the discrepancy between the simulation treating the framework as a perfect, infinite crystal as opposed to the flawed crystals which often exist in experimental crystals. The preparation of samples regarding the evacuation of guest molecules, removal of guest molecules inside the pores, and partial framework collapse all have an impact on the amount of adsorbent adsorbed.[86]

The surface area and pore volume simulations performed also use a GCMC method where a probe sphere is randomly inserted around each atom in the framework to test for overlap.[88] These results most closely agree with the BET method for experimentally calculating surface area using multilayer adsorption models.[89]

4.1.4 Goals of research

Armed with the knowledge of what makes a MOF a good candidate for hydrogen and methane adsorption, a MOF with an anticipated high hydrogen and methane adsorption capacity was designed. Based on the success of PCN-14, as well as both experimental and theoretical evidence, it stands to reason that increasing the number of aromatic rings in the ligand would result in an increase in both hydrogen and methane uptake. Both PCN-13 and PCN-14 contain an anthracene derivative as the ligand in the MOF with the difference between the two varying in the number of aromatic rings and the moiety of the carboxylates.

4.2 Results and discussion

In an attempt to improve the results of PCN-14, the ligand precursor 4,4'-(9,9'-bianthracene-10,10'-diyl)dibenzoic acid, a much larger ligand precursor than the ligand precursor used in PCN-14: 5,5′-(9,10-anthracenediyl)di-isophthalic acid, was synthesized as shown in Figure 9.

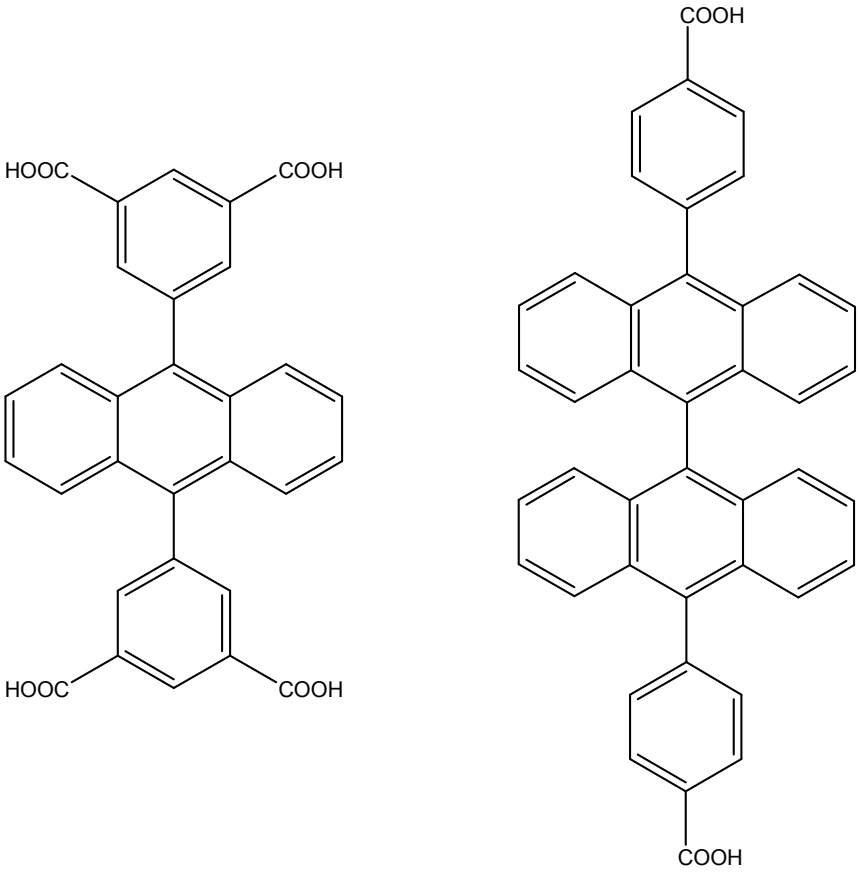

Figure 9. Ligand precursors of PCN-14 and PCN-80 respectively.

When allowed to react with $Zn(NO_3)_2 \cdot 6H_2O$ in dimethylacetamide with a small amount of HBF_4 for several days under solvothermal conditions, colorless block crystals of PCN-80 were formed. Single crystal X-ray diffraction was used to determine the atomic structure of the MOF (Table 2). The 3D framework interpenetrates itself three times resulting in a 25.59 x 25.68 x 25.87 Å framework. The result of the triple-interpenetration structure is shown in Figure 10. When viewed from the other axes it would appear that PCN-80 does not possess any dimensional channels as shown in

Figure 11. However, as shown in Figure 12, there exist channels that are 9.33 Å wide and vary in height from 4.77 – 6.16 Å.

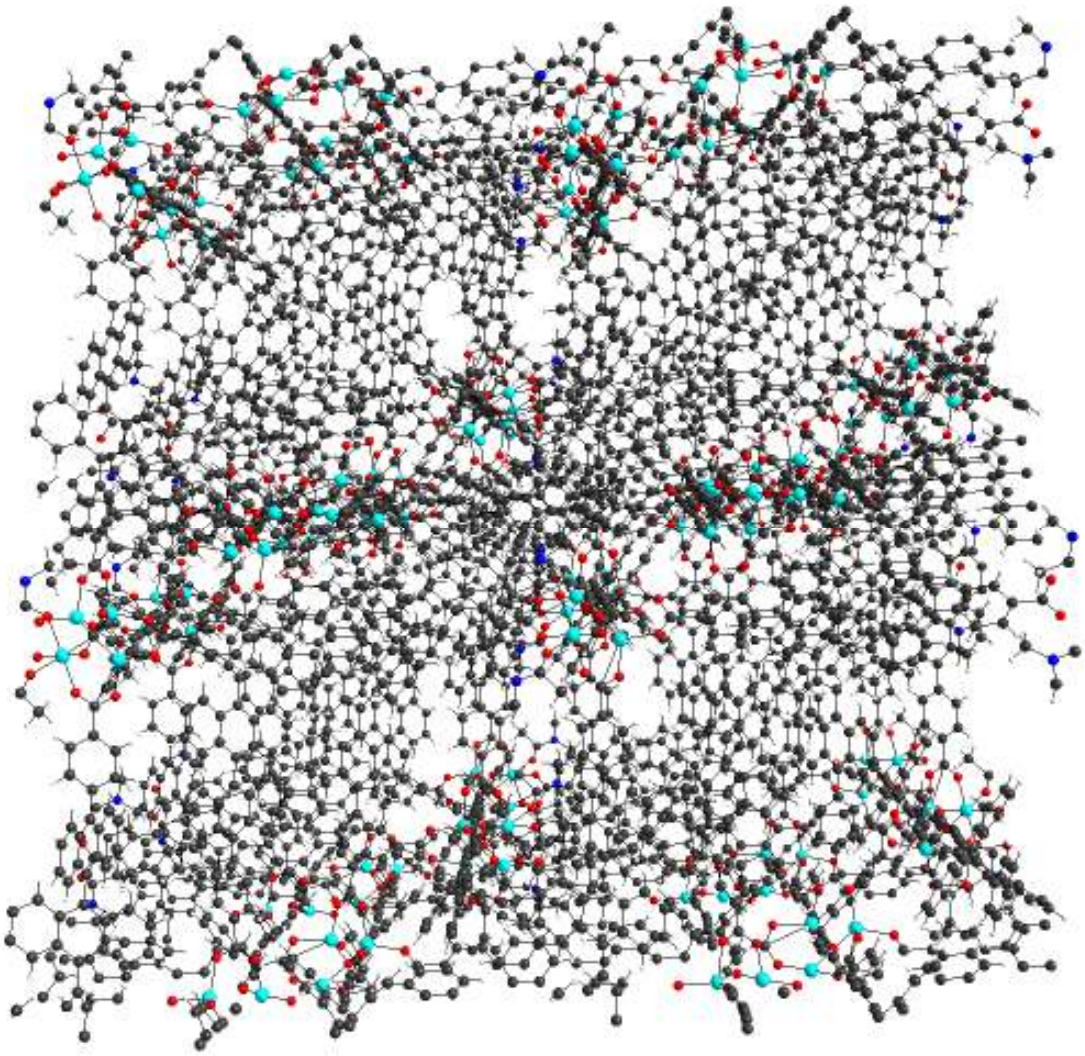

Figure 10. Extended structure of PCN-80 as viewed down the [1 0 0] direction.

Table 2. Crystal data, data collection, and structure refinement for PCN-80.

Identification code	PCN-80
Empirical formula	$C_{394}H_{252}N_4O_{43}Zn_{12}$
Formula weight	6514.44
Temperature	213(2) K
Wavelength	0.71073 Å
Crystal system	Triclinic
Space group	P -1
Unit cell dimensions	a = 25.586(15) Å, a= 91.596(7)° b = 25.675(15) Å, b= 93.763(8)° c = 25.869(15) Å, g = 103.323(7)°
Volume	16485(17) Å3
Z	1
Density (calculated)	0.656 Mg/m3
Absorption coefficient	0.464 mm-1
F(000)	3348
Crystal size	0.70 x 0.60 x 0.50 mm3
Theta range for data collection	1.87 to 25.91°.
Index ranges	-31<=h<=26, -31<=k<=31, -22<=l<=31
Reflections collected	101144
Independent reflections	62088 [R(int) = 0.1217]
Completeness to theta = 25.91°	96.70%
Absorption correction	Semi-empirical from equivalents
Max. and min. transmission	0.8012 and 0.7371
Refinement method	Full-matrix least-squares on F2
Data / restraints / parameters	62088 / 718 / 985
Goodness-of-fit on F2	1.034
Final R indices [I>2sigma(I)]	R1 = 0.1229, wR2 = 0.2490
R indices (all data)	R1 = 0.2670, wR2 = 0.2638
Largest diff. peak and hole	0.598 and -0.911 e.Å-3

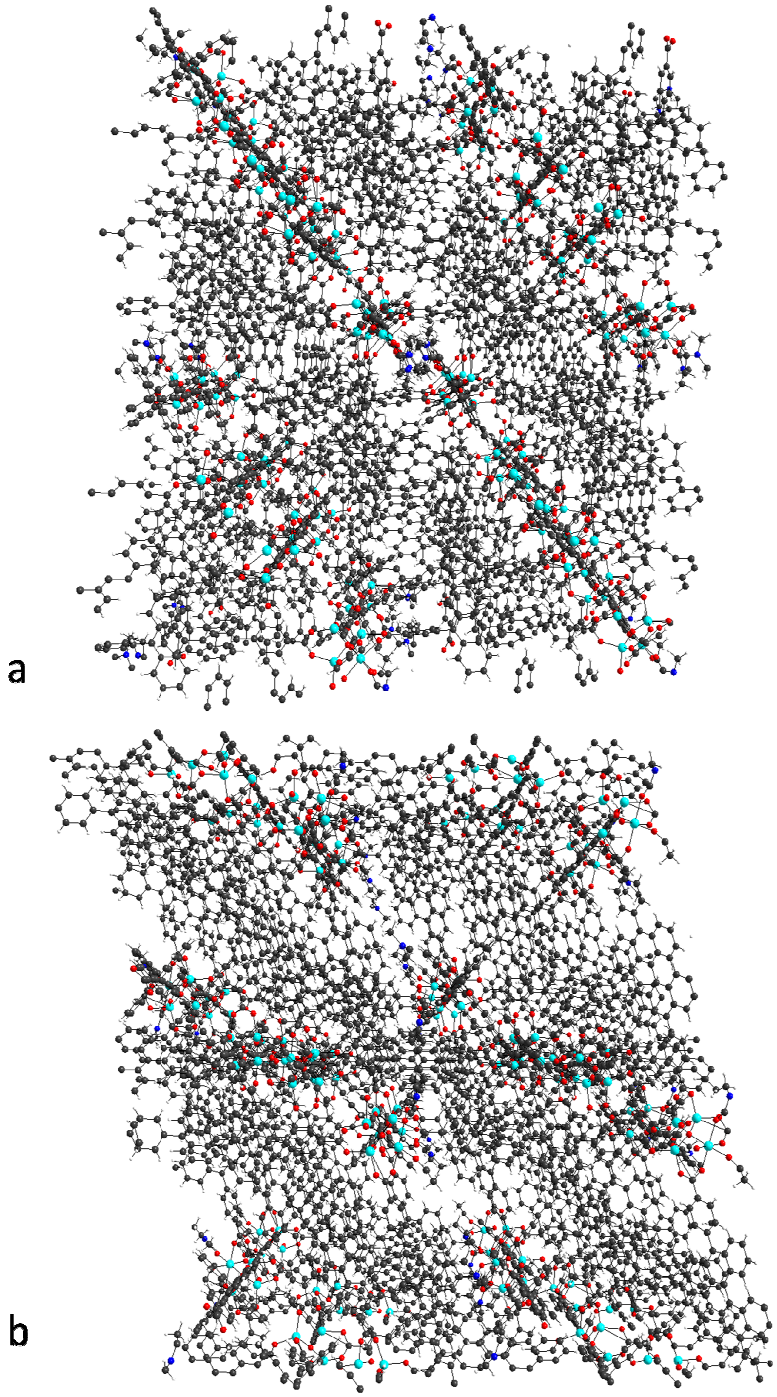

Figure 11. Extended crystal structure of PCN-80 viewed down the a) [0 1 0] and the b) [0 0 1] direction.

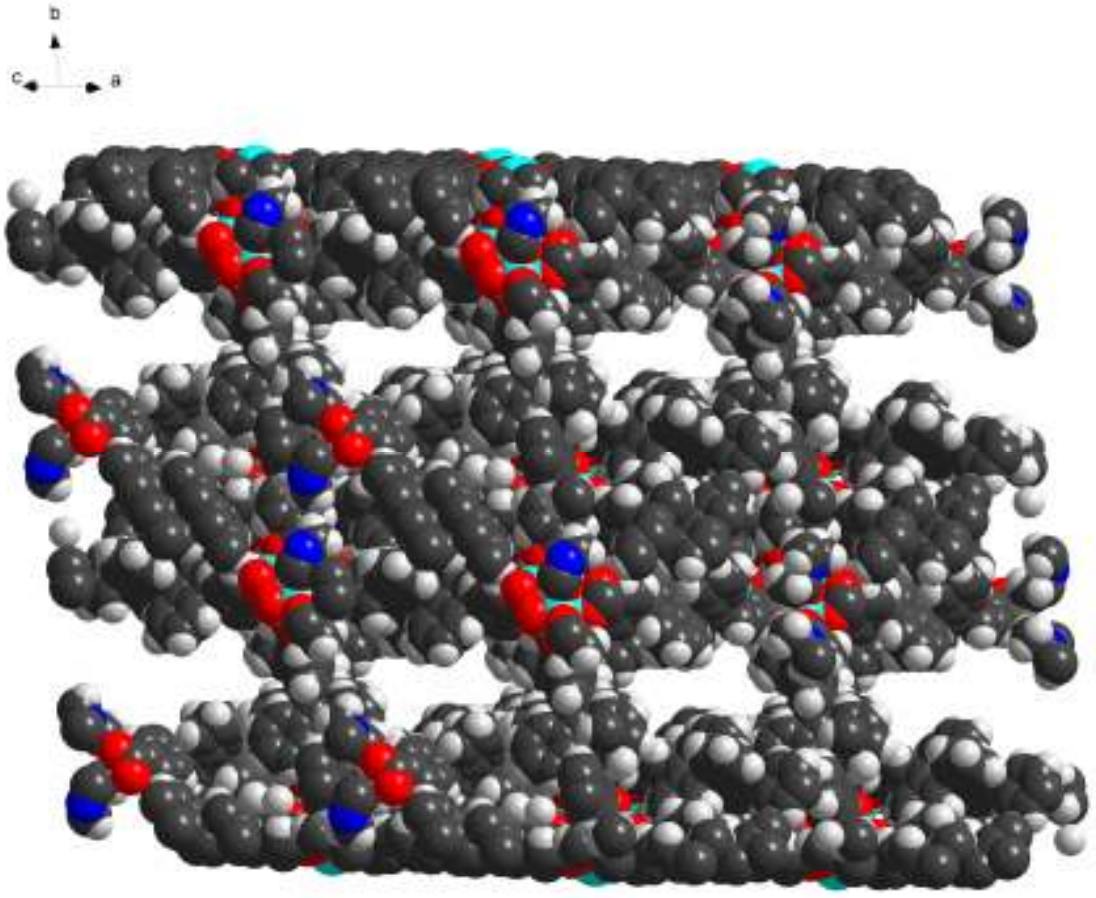

Figure 12. Space-filling model of PCN-80 indicating the presence of channels large enough for both hydrogen and methane gas to pass through.

PCN-80 crystallizes in the *P*-1 space group with a cell volume of approximately 1700 $Å^3$. PCN-80 is structurally unique as it possesses SBUs that display some rather uncharacteristic coordination geometries. Figure 13 shows the unit cell of PCN-80. Traditionally, each zinc atom in a Zn_4O is tetrahedral in geometry, as shown in Figure 14. Within this cell, there exist unique SBUs in which one of the Zn atoms possesses a nearly perfect octahedral coordination environment as shown in Figure 15. To the best of

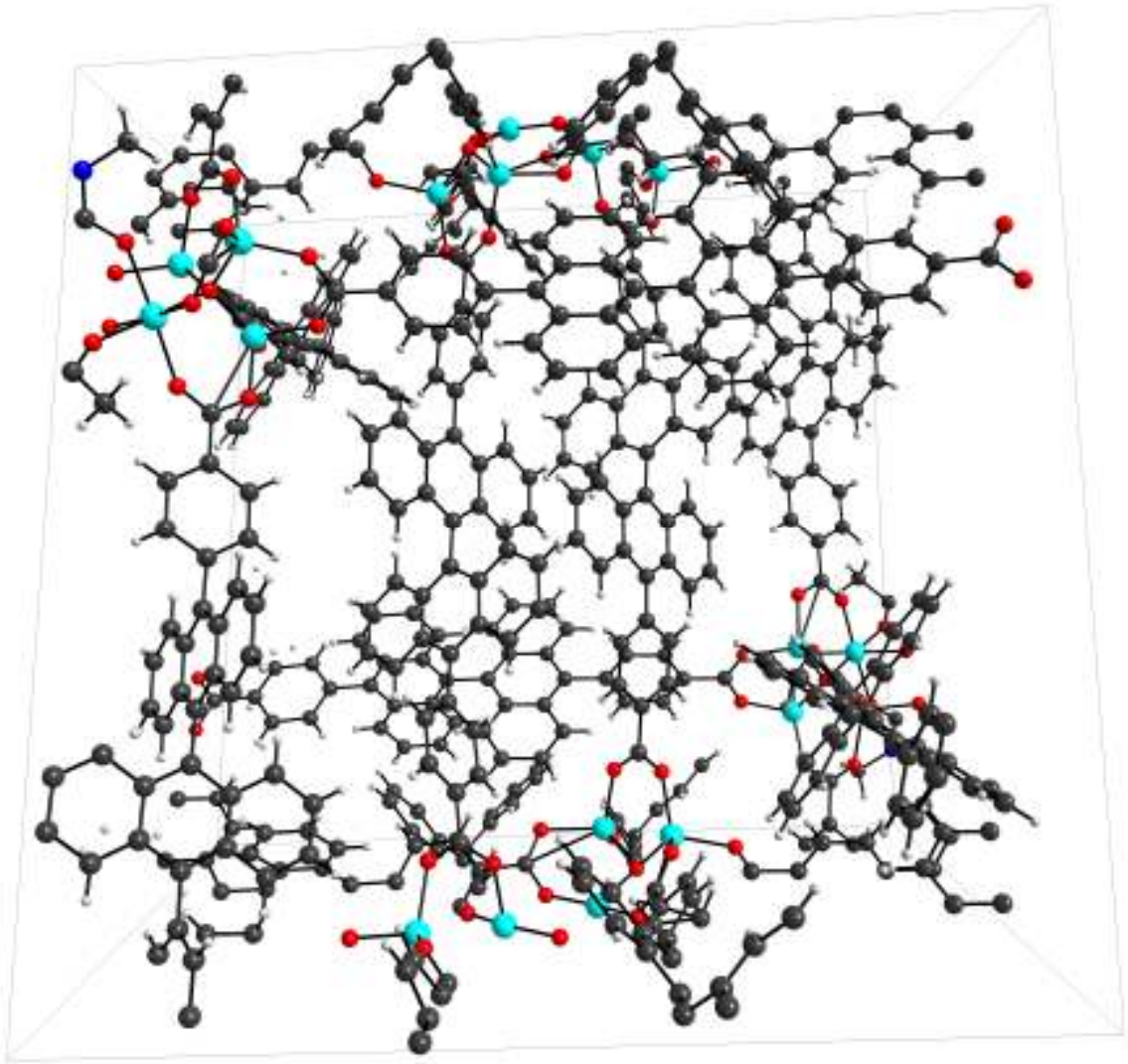

Figure 13. Unit cell of PCN-80 viewed down the [1 0 0] direction (non-coordinated solvent molecules removed for clarity.

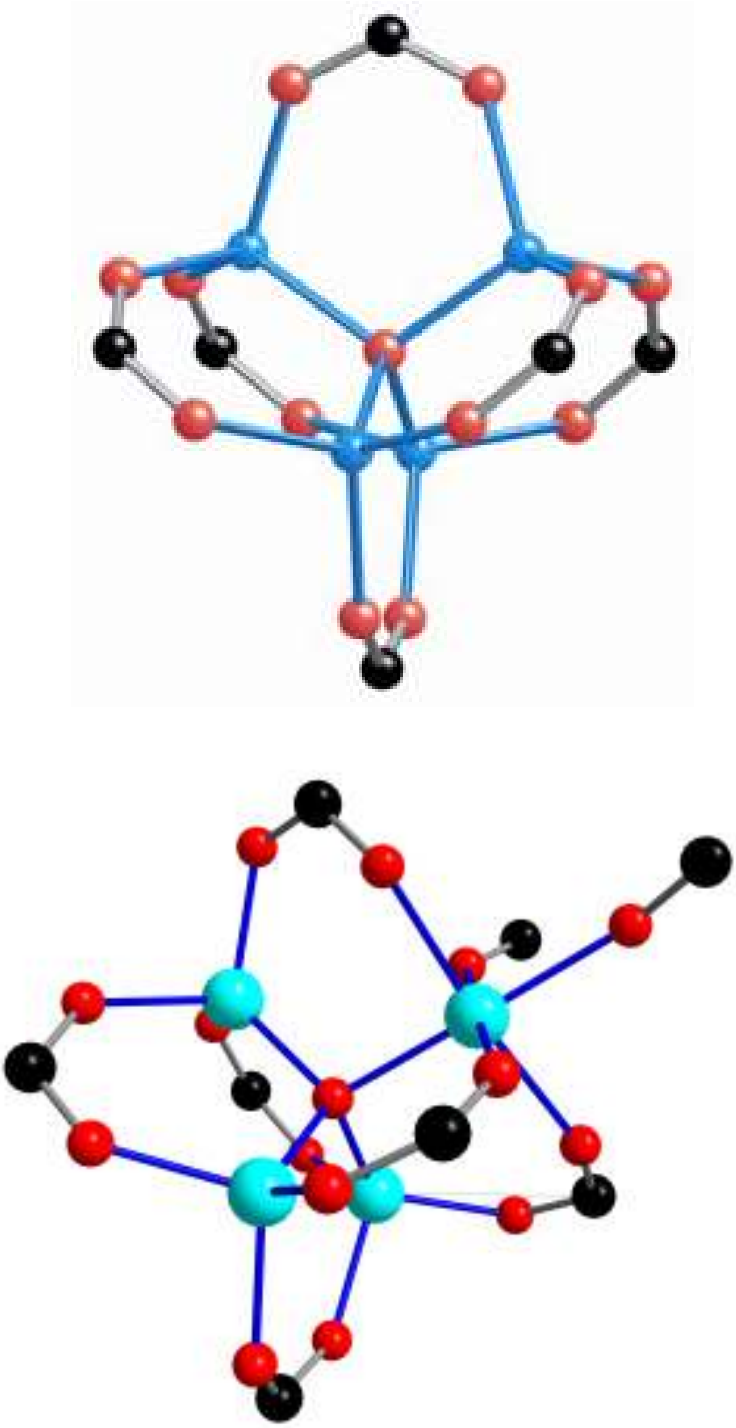

Figure 14. Traditional $Zn_4(O)(CO_2)_6$ SBU compared to the Zn_4O SBU of PCN-80.

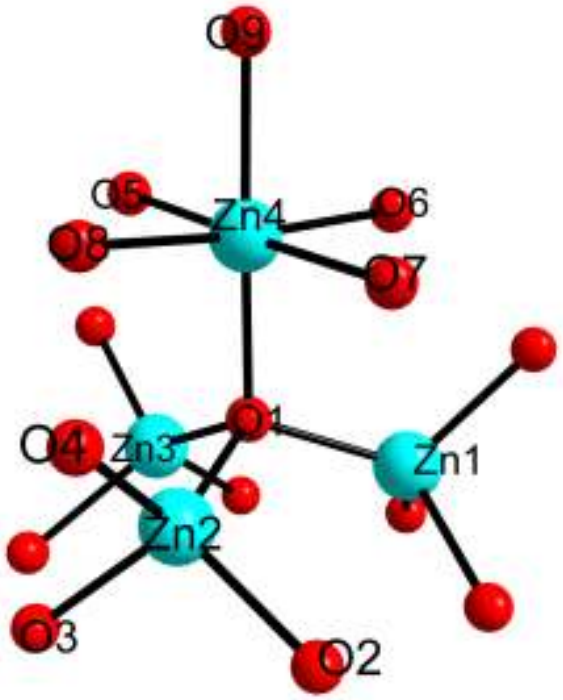

Figure 15. Unique SBU of PCN-80. All carbons and hydrogens removed for clarity; oxygen atoms numbered on Zn 2 and Zn 4 to display the traditional tetrahedral and unique octahedral geometries, respectively; selected bond lengths (Å) and angles (deg.) O(1)-Zn(1) 1.882(1), O(1)-Zn(2) 1.952(9), O(1)-Zn(3) 1.911(1), O(1)-Zn(4) 2.027(9), Zn(2)-O(2) 1.970(7), Zn(2)-O(3) 1.946(8), Zn(2)-O(4) 1.967(6), Zn(4)-O(5) 2.045(9), Zn(4)-O(6) 2.099(1), Zn(4)-O(7) 2.164(1), Zn(4)-O(8) 2.107(1) Zn(4)-O(9) 2.075(1), Zn(4)-O(1)-Zn(1) 109.66(2), Zn(1)-O(1)-Zn(2) 109.35(2), Zn(2)-O(1)-Zn(3) 107.68(2), Zn(3)-O(1)-Zn(4) 113.70(2), O(1)-Zn(2)-O(2) 110.93(2), O(2)-Zn(2)-O(3) 105.95(2), O(3)-Zn(2)-O(4) 99.71(2), O(4)-Zn(2)-O(1) 122.73(2), O(1)-Zn(4)-O(8) 95.43(2), O(8)-Zn(4)-O(5) 89.69(2), O(5)-Zn(4)-O(6) 93.06(2), O(6)-Zn(4)-O(7) 88.00(2), O(7)-Zn(4)-O(8) 89.06(2), O(9)-Zn(4)-O(6) 89.52(3), O(9)-Zn(4)-O(1) 178.39(2), O(8)-Zn(4)-O(6) 173.53(2), O(5)-Zn(4)-O(7) 177.78(2).

the author's knowledge, this is the first example of a Zn_4O SBU that possesses an octahedral Zn atom. In this SBU, three Zn atoms adopt the Zn_4O geometry while one of the Zn atoms adopts that of a Zn paddlewheel.

The 4,4'-(9,9'-bianthracene-10,10'-diyl)dibenzoate ligand adopts a unique twist between the anthracene rings in the structure of PCN-80. The crystallized form of 9,9-bianthraceneyl adopts an almost perfect twist of 90° between the two anthracene chains.[90] In close accordance with this is the 86.16° twist between the anthracene chains in 4,4'-(9,9'-bianthracene-10,10'-diyl)dibenzoate of PCN-80. The similarities between the two linkers can be viewed in Figure 16. The length of the ligand, which is over 18.5 Å from carboxylate carbon to carboxylate carbon through space (Figure 16), is extremely long for a linear, ditopic ligand. This is the primary cause of the three-fold interpenetration of PCN-80. However, the fact that the ligand was not significantly altered indicates that in the absence of a three-fold interpenetration, PCN-80 would most likely possess a rigid, robust framework.

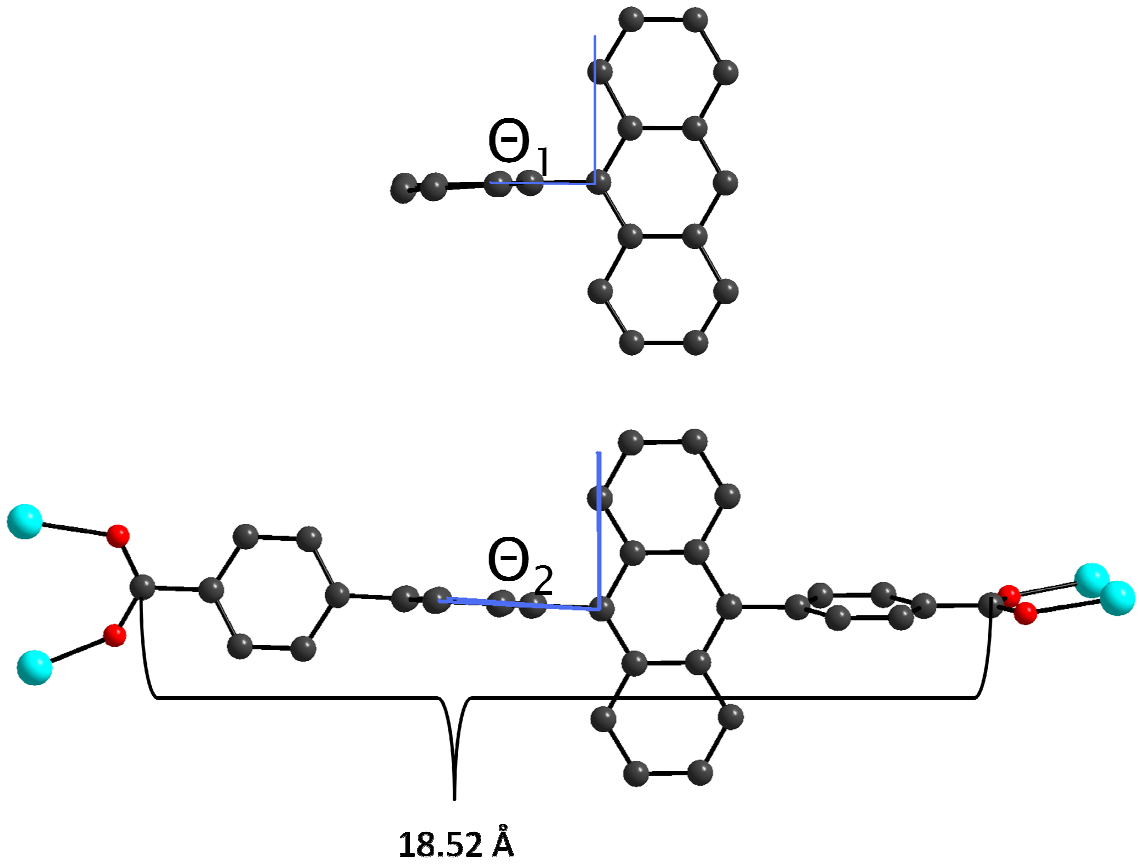

Figure 16. 9,9'-bianthraceneyl and 4,4'-(9,9'-bianthracene-10,10'-diyl)dibenzoate twist angles between the anthracene rings (hydrogens removed for clarity) (Θ_1 = 90.88°, Θ_2 = 86.16°).

Gas adsorption measurements were attempted, yet the crystal is not stable when exposed to the air. This decomposition can be attributed to the exposure to atmospheric water which results in an amorphous product. X-ray powder studies on crystals containing Zn_4O SBUs verify this decomposition by the appearance of new peaks in

powder patterns after atmospheric exposure ranging from 10 minutes to 24 hours.[91] Anaerobic preparation of crystal samples enables the stability required to perform such measurements, yet has not been carried out to date.

In order to gain a better understanding of the potential properties of PCN-80, molecular simulations using Materials Studio 5.0 were conducted to determine surface area, pore volume, and adsorption capacities.. The molecular simulation revealed a surface area of 3801 m^2/g with a crystal density of 0.656 g/cm^3. The pore volume was calculated to be 0.74 cm^3/g; this volume is rather high considering the three-fold interpenetration and bulkiness of the ligand. Figure 17 shows the simulated hydrogen adsorption isotherm from 0 to 101.33 kPa at 77 Kelvin. The type I behavior indicates a microporous framework while the maximum adsorption of 258.65 units of hydrogen per molecular unit of PCN-80 correlates to a gravimetric hydrogen adsorption of 7.43 weight percent; this correlates to a volumetric loading capacity of 61.47 g/L. Although these calculations were performed at 77 K, PCN-80 surpasses the gravimetric and volumetric storage targets for 2010, 6 weight percent and 45 g/L, respectively.

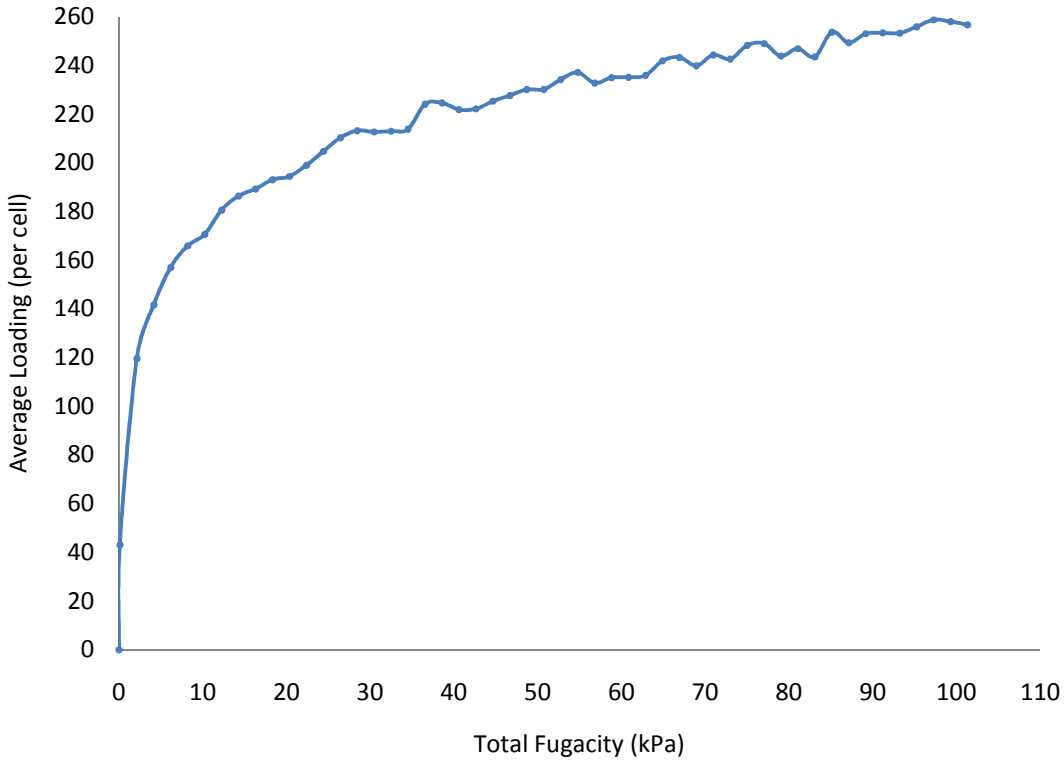

Figure 17. Simulated H_2 adsorption isotherm for PCN-80.

The simulation performed in Materials Studio 5.0 also identified the location of the adsorbed gases. The high hydrogen adsorption capacity of PCN-80 is a direct result of the structure of PCN-80. As shown in Figure 18. Continued

b) on page 55, a good deal of the adsorbate is located around the Zn metal cluster, as is customary for MOF-based adsorbents. The hydrogen is also focused around the center of the bianthryl center of the ligand, which supports the claim that an increase in aromatic rings increases the adsorption of hydrogen. The fact that interpenetration in the frameworks PCN-6 and PCN-9 improved the hydrogen adsorption capacity may also explain the high adsorption capacity of PCN-80, as it is triply interpenetrated as opposed

to the doubly interpenetrated networks of PCN-6 and PCN-9.[92,93] The relatively high heat of adsorption of 10.14 kJ / mol at 101.33 kPa not only ranks among the highest of reported MOFs but also indicates the strong attraction between the hydrogen and the framework.

a) 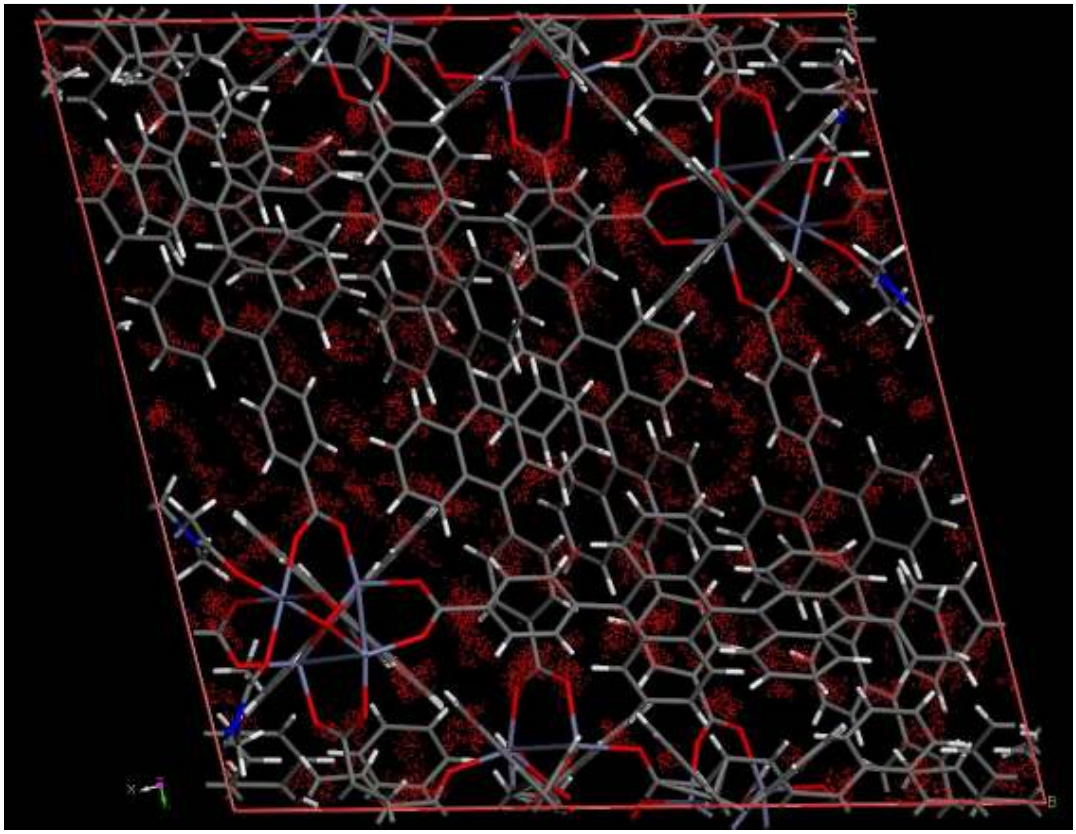

Figure 18. a) Simulated H_2 adsorbate location at 101.33 kPa and b) space-filling model of the hydrogen in the channel of PCN-80.

b) 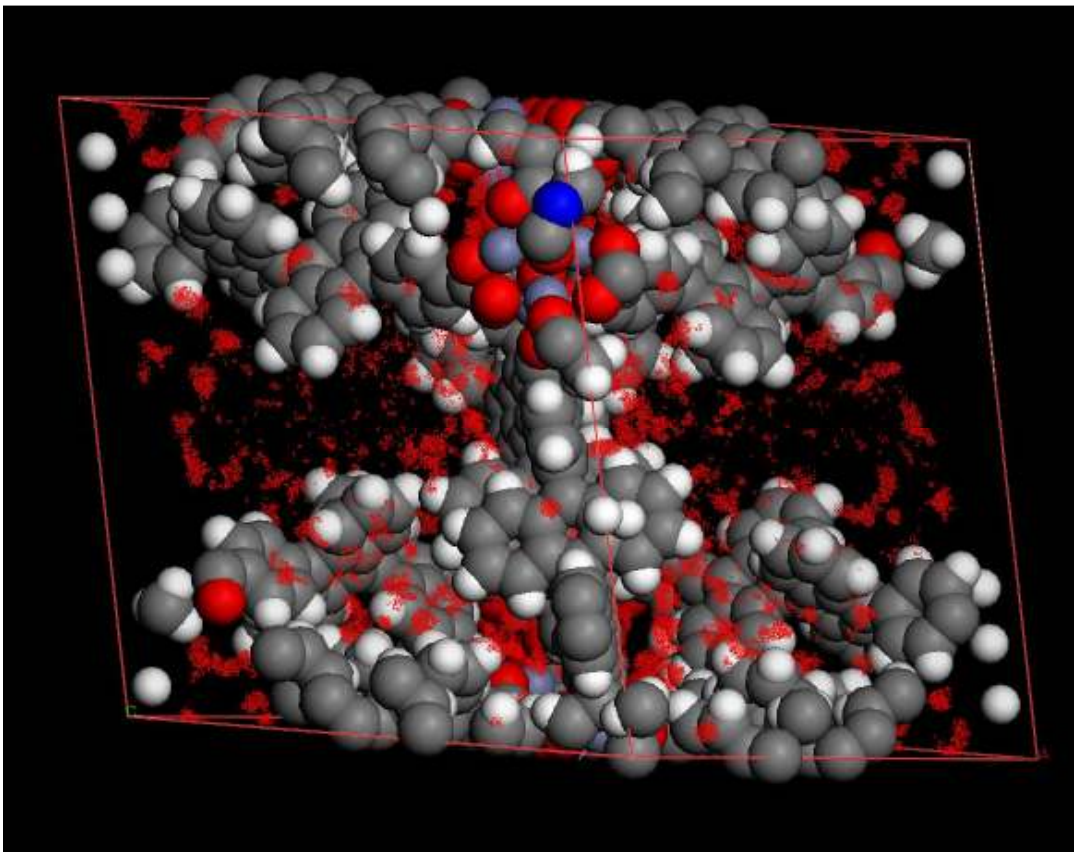

Figure 18. Continued

As a result of the exceptionally high hydrogen uptake at low pressure, a high pressure adsorption isotherm was simulated on Materials Studio 5.0; the isotherm conditions were set at 77 K while the pressure was varied from 0 – 10000 kPa. As shown in Figure 19, the adsorption continues to gradually rise at pressures as high as 10000 kPa (100 bar), a pressure still deemed as safe for on-board hydrogen storage.[67] Reaching a maximum storage of 9.20 weight percent (75 g/L) PCN-80 ranks among the highest in percent

weight hydrogen adsorbed and, to the author's knowledge, possesses the highest volumetric storage capacity of all MOF materials at high pressure.

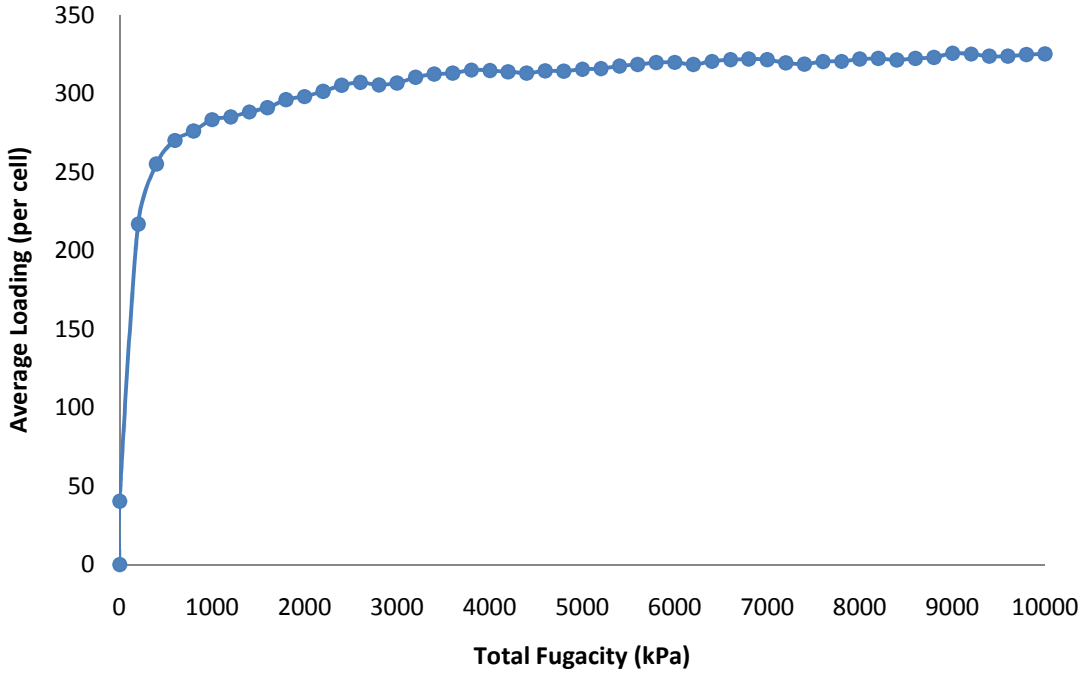

Figure 19. Simulated high pressure hydrogen adsorption isotherm for PCN-80.

Figure 20 shows the isosteric heats of adsorption for hydrogen as a function of weight percent of hydrogen adsorbed by PCN-80 at high pressure. The Q_{st} initially decreases sharply and then slowly increases. This indicates that at higher pressures, the framework still has a strong attraction to the adsorbed hydrogen; this also shows that the hydrogen is not merely "trapped" yet is interacting with the framework. This is more than likely a combined effect of the high surface area, eight aromatic rings of the ligand, and the three-fold interpenetration, all elements which have been proposed to increase the

adsorption of hydrogen.[1,16,25,67] These attributes associated with high pressure adsorption, as well as those at ambient pressure, makes PCN-80 quite an attractive candidate for hydrogen storage.

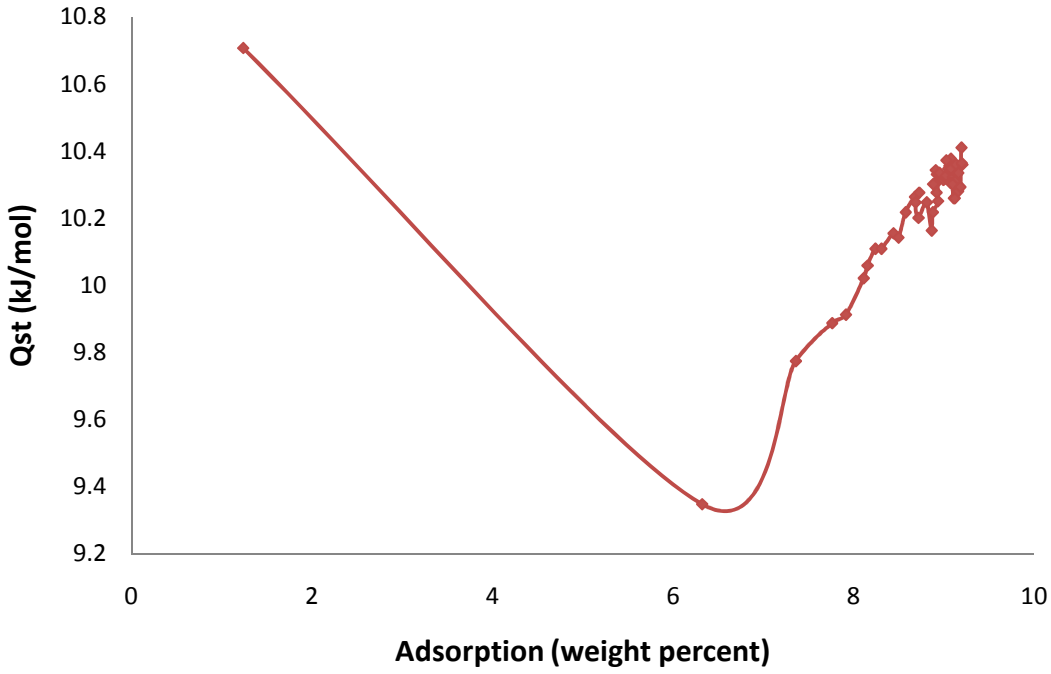

Figure 20. Isosteric heats of adsorption for hydrogen.

Figure 21 displays the simulated isotherm for methane adsorption at 298 K from 0 to 101.33 kPa resulted in a maximum adsorption of 45 units of methane per molecular unit of PCN-80. This corresponds to a maximum uptake of 9.59 weight percent. This methane adsorption corresponds to a volumetric uptake of 78.47 g/L, which is equivalent to 97.09 v/v at standard pressure and temperature. Although the weight percent of methane stored is on the higher range of MOFs, the v/v uptake is 44% of that of PCN-14

(220 v/v).[1,82] However, PCN-14 adsorbed 220 v/v at 35 bar; PCN-80 was examined only at low pressures.

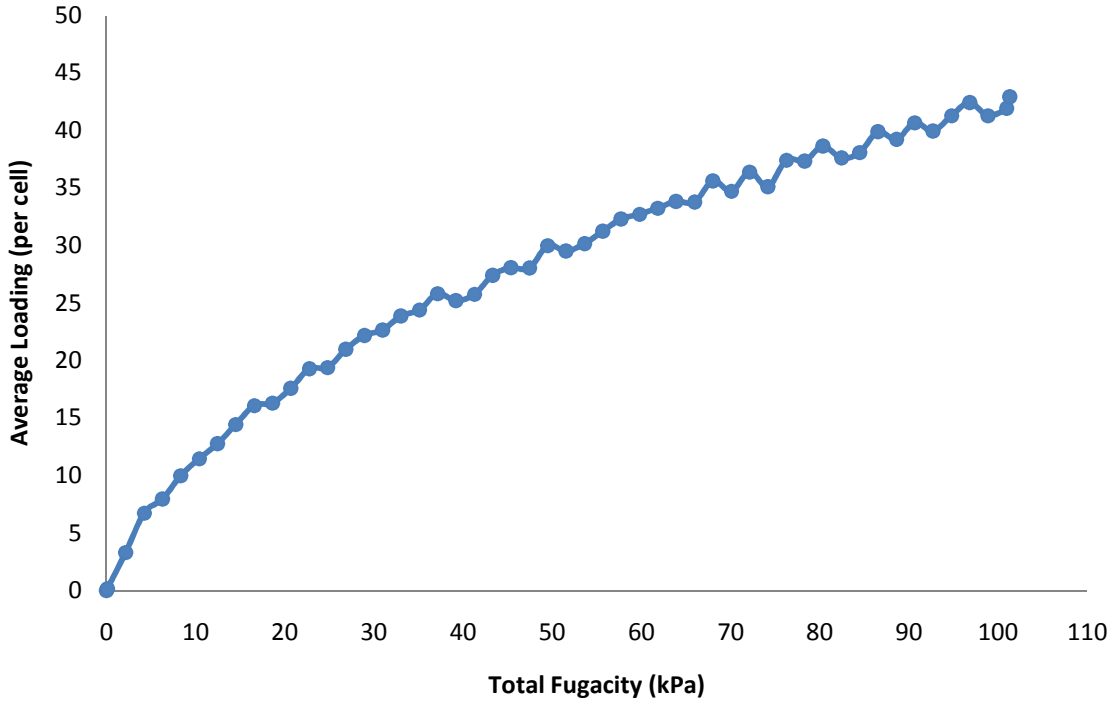

Figure 21. Simulated methane adsorption isotherm for PCN-80.

The methane adsorption simulation revealed that PCN-80 possesses an isosteric heat of adsorption of 27.93 kJ/mol. This value is among the highest reported for MOFs and to the author's knowledge, is exceeded only by PCN-14, the record holder for methane adsorption in a MOF. Additionally, this lends further validity to the notion that an increase in the number of aromatic rings of the ligand increases the affinity of the framework for methane.[77,82,94]

4.3 Future work

The next immediate step that needs to occur is the air-sensitive workup of a crystal of PCN-80 to prevent contact with the atmosphere. This would prevent the decomposition of the crystals that is preventing the necessary experimental isotherm data. The PCN-80 crystals can be worked up in a glovebox; the solvent exchange can take place with dry, anhydrous solvents and the crystals can be charged in a Schlenk flask and transferred to a vacuum line to remove solvent and guest molecules, thus completely isolating the crystals from any exposure to oxygen.

Crystals obtained by the solvothermal reaction of $BADBA^{2-}$ with $Cu(NO_3)_2 \cdot 2.5H_2O$ are highly desirable for two reasons: Cu frameworks are usually more stable, and Cu MOFs have been shown to possess a higher adsorption capacity for hydrogen.[95] To prevent decomposition when exposed to the atmosphere, as well as to increase hydrogen adsorption capacity, efforts have been taken to form a framework with the $BDBA^{2-}$ ligand and $Cu(NO_3)_2 \cdot 2.5H_2O$. Thus far, crystals have yet to be obtained as reaction conditions have only resulted in powder precipitate. Further reaction conditions must be tested using a high-throughput method in order to obtain a suitable single crystal. Once obtained, the crystal should possess the $Cu_2(CO_2)_4$ paddlewheel SBU. With this, the crystal is expected to be stable to atmospheric conditions and an experimental isotherm will be available to determine surface area, adsorption capacity, and the size of the pore opening, should the structure possess an accessible cage. More so, assuming axial coordination to the Cu atoms by solvent or guest molecules, removal of the guests

should result in a SBU with open metal sites on the axial positions of the Cu atoms, thus further enhancing the binding ability as previously explained.

Perhaps the most anticipated result concerning the bianthryl systems involves the ligand precursor 4,4'-(9,9'-bianthracene-10,10'-diyl)di-isopthalate as it's isopthalic moiety is a true isoreticular extension of the ligand used in PCN-14, (9,10-anthracenediyl)di-isophthalate. This ligand precursor has been isolated and characterized, yet to date no crystals have resulted from the reaction with either Cu or Zn salts. The resultant MOF should form the paddlewheel SBU as the isophthalic moiety lends itself to form paddlewheel SBUs.[82] By increasing the length of the ligand, it stands to reason that the surface area will also increase. As shown with PCN-80, the attractive forces between the hydrogen and the aromatic rings results in localization of the gas around the ligand even in light of an absence of cages and channels in the framework. The increase in surface area should result in an even higher adsorption of hydrogen.

4.4 Synthesis

Synthesis of 9,9'-bianthryl:

9,10-Anthracenedione (5.00 g, 24.0 mmol) and a stirbar were charged in a 200 mL roundbottom flask. Mossy tin (20 g, 166.80 mmol) was cut up into small pieces and added to the flask. Glacial acetic acid (50 mL) was added and the solution was heated to reflux. When reflux was achieved, a delivery funnel was attached and 35 mL of hydrochloric acid was added dropwise to the solution over a period of two hours. Upon completion of the acid delivery, the heat was turned off and the reaction was stirred over

night. The next day, the precipitate was filtered off and recrystallized in hot toluene. The hot solution was filtered to remove chunks of tin and allowed to cool in the freezer. Greenish-yellow crystals appeared after two days and were isolated. Yield: 25.91% (2.20 g, 6.21 mmol) ^{1}H NMR (DMSO-d_6): δ 8.87 (s, 2 H), δ 8.25(d, J = 8.4 Hz, 4 H), δ 7.49 (t, J = 7.2 Hz, 4 H), δ 7.18 (m, 4 H), δ 6.89 (d, J =8.7 Hz, 4 H).

Synthesis of 10,10'-Dibromo-9,9'-bianthryl:

9,9'-bianthryl (1.8 g, 5.08 mmol) was charged in a 500 mL round-bottom flask dissolved in 100 mL of dichloromethane with the aid of a stirbar and heat. The flask was stirred vigorously and cooled to 0 °C and a solution of bromine (0.6 mL, 11.79 mmol) in 100 mL of dichloromethane was added dropwise over a period of two hours with the aid of an open delivery funnel. The reaction was allowed to warm to room temperature and stirred overnight. The following day, the solvent was removed via rotavap and approximately 150 mL of ethanol was added. The solution was brought to reflux and refluxed for one day to remove impurities. The precipitate was filtered and collected to yield pure yellow flakes of 10,10-dibromo-9,9'-bianthryl. Yield: 46.63% (1.21 g, 2.37 mmol) ^{1}H NMR (DMSO-d_6): δ 8.62 (d, J = 9.0 Hz, 4 H), δ 7.69 (t, J = 8.1 Hz, 4 H) δ 7.29 (t, J = 6.9 Hz, 4 H) δ 6.95 (d, J = 8.7 Hz, 4 H).

Synthesis of 4,4'-(9,9'-bianthracene-10,10'-diyl)dimethylbenzoate:

10,10'-Dibromo-9,9'-bianthryl (2.61 g, 5.12 mmol), 4-methoxycarbonyl)phenylboronic acid (2.85 g, 15.83 mmol), sodium carbonate (1.63 g,

15.38 mmol), and tetrakis(triphenylphosphine)palladium(0) (0.42 g, 0.36 mmol), and a stir bar were charged in a 250 mL round bottom Schlenk flask fitted with a condenser. The flask was filled with nitrogen and evacuated three times. 50 mL of tetrahydrofuran, 50 mL of toluene, and 17 mL of water were combined in a flask, degassed, and transferred to the reaction flask. The mixture was heated to reflux and the reaction was stirred for one day. The following day, the reaction was quenched with water and the crude product was extracted three times with diethyl ether. The organic layer was washed with water followed by brine. The crude product was separated by column chromatography from an ethyl acetate / hexane mixture ranging from 5 – 50%. The pure product was the last to elute and was collected as a bright yellow solid. Yield: 81.9% (2.61 g, 4.19 mmol) ^{1}H NMR (DMSO-d_6): δ 8.32 (d, J = 9.00 Hz, 4 H), δ 7.83 (d, J = 7.35 Hz, 4 H), δ 7.67 (d, J = 9.00 Hz, 4 H), δ 7.45 (t, J = 7.80 Hz, 4 H), δ 7.29 (t, J = 6.60 Hz, 4 H), δ 7.07 (d, J = 8.7 Hz, 4 H), δ 3.99 (s, 6 H).

Synthesis of 4,4’-(9,9’-bianthracene-10,10'-diyl)dibenzoic acid:

4,4'-(9,9'-bianthracene-10,10'-diyl)dimethylbenzoate (0.107 g, 0.172 mmol) and sodium hydroxide (0.17 g, 4.25 mmol) were dissolved in 10 mL of water and stirred overnight at 50 °C. The following day, the mixture was cooled, filtered to remove the inorganic solids, and acidified with hydrochloric acid. The hydrolysis produced a bright yellow solid which was filtered, dried in an oven, and determined pure.

Yield: 74.4% (0.076 g, 0.13 mmol) ^{1}H NMR (DMSO-d_6): δ 13.18 (s, OH), δ 8.29 (d, J = 8.4 Hz, 4 H), δ 7.79 (d, J = 8.4 Hz, 4 H), δ 7.69 (d, J = 9 Hz, 4 H), δ 7.46 (t, J = 8.1 Hz, 4 H), δ 7.29 (t, J = 8.7 Hz, 4 H), δ 7.09 (d, J = 8.7 Hz, 4 H).

Synthesis of PCN-80:

Employing a reaction ratio of 3 : 1 metal to ligand ratio: 7.00 mg of $Zn(NO_3)_2 \cdot 6H_2O$ and 4.60 mg of H_2BADBA were dissolved in 1.5 mL of DMA and 1 drop of tetrafluroboric acid in a small, 0.5 dram vial. The vessel was sonicated to ensure complete mixture and then placed in an oven at 85 °C for seven days. Clear, block crystals which decomposed (confirmed by visual cracking of crystals when viewed under a microscope) were isolated and characterized by single crystal X-ray diffraction.

CHAPTER V

SYNTHESIS OF TWO-DIMENSIONAL FRAMEWORK AND RELATIONSHIP BETWEEN AROMATIC RINGS AND FRAMEWORK PROPERTIES

5.1 Introduction and research objectives

Following the synthesis of PCN-80, an interest was taken in what properties will result in a framework when the number of aromatic rings present in the ligand is increased. Starting with 1,4 benzenedicarboxylic acid, a comparison can be made as to the effects of systematically extending the ligand from a benzene to a naphthalene to an anthracene to a bianthryl and finally to an extended bianthryl ligand as shown in Figure 22. By utilizing a linear, ditopic ligand, the formation of a framework is guaranteed. Comparing the effects of extending the aromatic rings contained in the ligand with respect to surface area, pore opening and volume, and gas uptake will lend insight as to exactly how to optimize these ditopic ligands for the most desirable properties. To alleviate the effect of the metals on the properties of these selected MOFs as much as possible, all MOFs used in the following were synthesized with zinc salts. The SBU that is formed is a factor of synthetic conditions as well as kinetic and thermodynamic factors that are beyond the scope of control for this study.

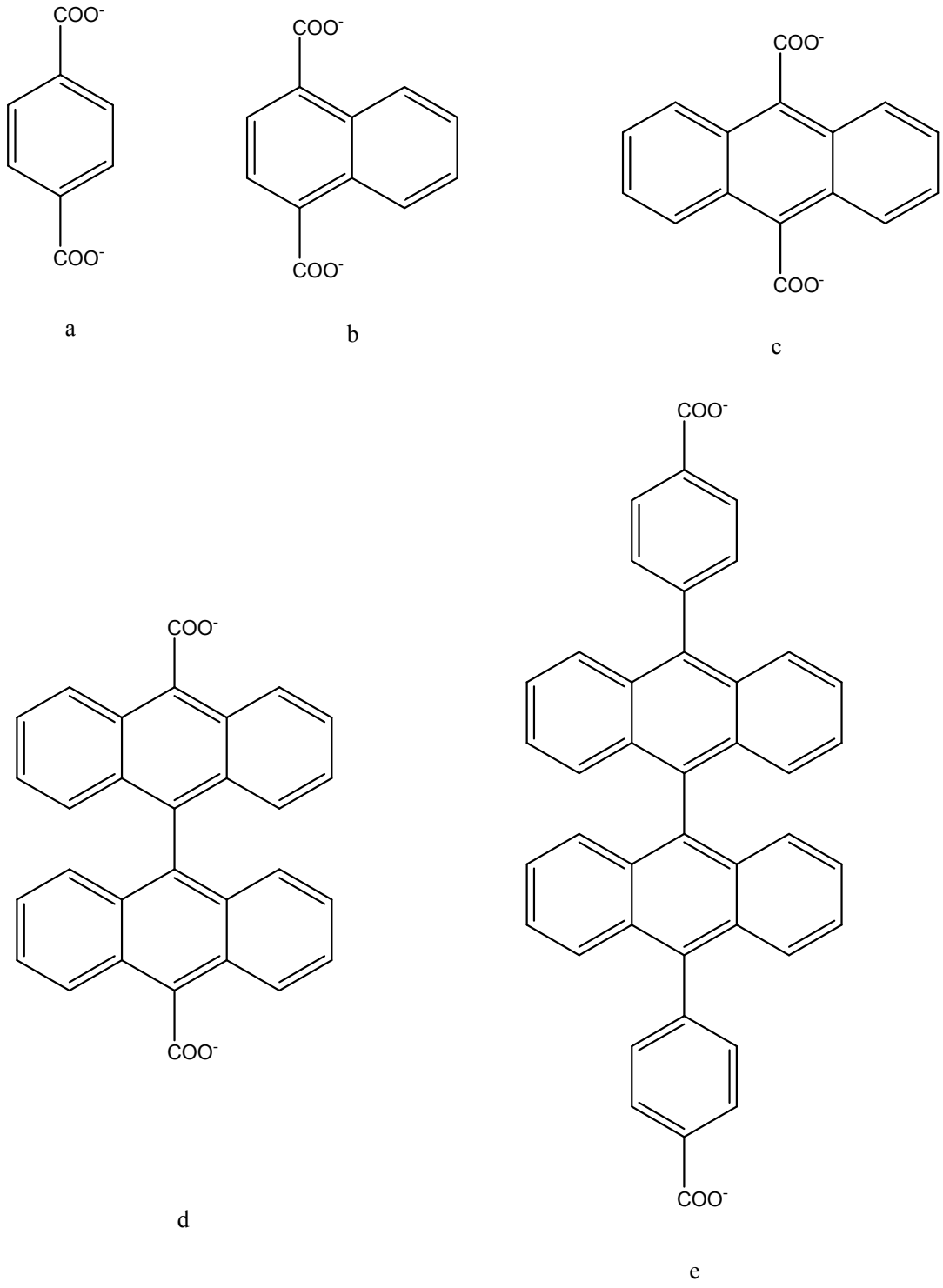

Figure 22. Stepwise growth of linear, ditopic ligands: a) BDC^{2-} b) NDC^{2-} c) ADC^{2-} d) $BADC^{2-}$ e) $BADBA^{2-}$.

5.2 Results and discussion

1,4-benzenedicarboxylicacid (H_2BDC) was the ligand utilized by the Yaghi lab in the formation of the most infamous MOF to date. The diffusion of triethylamine into a solution of H_2BDC and $Zn(NO_3)_2$ in a mixture of DMF and chlorobenzene with a small amount of H_2O_2 resulted in the formation of $Zn_4O(BDC)_3 \cdot (DMF)_8(C_6H_5Cl)$, otherwise known as MOF-5.[60] In this structure, Zn_4O inorganic clusters are connected to an octahedral array of BDC groups to form the $Zn_4(O)(CO_2)_6$ SBU.[96] The connection of the ligand and SBU creates square openings that form two distinct cages which are differentiated by the orientation of the aromatic rings. One cage has all of the faces of the aromatic rings facing towards the center of the pore whereas the other cage has the edges of the aromatic rings pointing towards the pore.[97] The window openings for MOF-5 are approximately 7.8 Å at temperatures below 298 K.

The physical properties and adsorption data for MOF-5 has been met with scrutiny.[16] Originally, the authors estimated the Langmuir surface area to be 2900 m^2/g.[60] Later studies by the same researchers found the Langmuir surface area to be 4171 m^2/g.[98] Deviations in the range of 1014 to 4400 m^2/g exist in the literature.[16,99,100] Likewise, the BET surface areas have been reported in the range from 572 to 3800 m^2/g.[99,100] The H_2 adsorption data at 77K and 1 atm is fairly agreeable with the highest reported value being 1.32 wt%.[100] These discrepancies exist as a result of varying sample preparations as the Zn_4O core is known to be high sensitive to atmospheric moisture and exposure may result in an unstable framework thereby yielding unreliable data.[91]

While retaining the linear, ditopic moiety, the Yaghi group used 1,4 napthalenedicarboxylic acid (H_2NDC) as an isoreticular ligand. The vapor diffusion of a solution of H_2O_2 and a chlorobenzene – triethylamine mixture into a solution of DMF and chlorobenzene containing $Zn(NO_3)_2 \cdot 6H_2O$ and H_2NDC yielded MOF-48.[101] Having the molecular formula, $Zn_6(NDC)_5(OH)_2(DMF)_2 \cdot 4DMF$, MOF-48 contains a hexameric building block SBU; ten NDC units bridge the Zn centers in a dimonodentate fashion.[101] This three-dimensional framework possesses one-dimensional channels with an opening of 6.2 Å in diameter.[101] MOF-48 has the same general structure of MOF-5 with simulated calculations revealing a pore diameter of approximately 13.6 Å.[61] MOF-48 has the same pore dimensions as MOF-5, yet the windows allowing access to the pores are diminished by the presence of the additional aromatic ring the naphthalene. When in the most optimal, sterically favored position with two of the naphthalenes on opposite sides of the window are directed towards the window. This creates a window opening of approximately 2.1 Å compared to 7.8 Å for MOF-5.[97] No experimental BET surface area, pore volume, or gas adsorption measurements are reported in the literature, presumably due to the high degree of instability of the MOF.

To add one more aromatic ring while keeping the same linear, ditopic carboxylic acid scheme results in the ligand precursor 9,10-anthracenedicarboxylic acid (H_2ADC). It had been predicted that H_2ADC would form a three-dimensional MOF, the theoretical MOF-993, with Zn_4O cluster SBUs that would have exceptional methane storage capacity and a high heat of adsorption.[77] The actual reaction between H_2ADC and $Zn(NO_3)_2 \cdot 6H_2O$ under solvothermal conditions produced light-brown crystals of PCN-13 with the formula $Zn_4O(H_2O)_3(C_{16}H_8O_4)_3 \cdot 2DMF$.[102] As theorized by Snurr et al., this MOF contains the Zn_4O metal cluster at its metal center. However, PCN-13 contains an unusually distorted SBU in which only one of the zinc atoms is four-coordinated while the other three are five-coordinated; more so, the three five-coordinated zinc atoms are aligned forming an overall trigonal pyramidal geometry as opposed to the traditional tetrahedral center normally associated with $Zn_4O(COO)_6$ SBUs.[102] This distortion is brought on by the bulkiness of the ADC ligand which opens a previously inaccessible coordination site that an aqua ligand occupies, thus forming a distorted trigonal bipyramidal geometry around the basal zinc atoms.[102] No interpenetration exists within the framework despite the bulkiness of the ligand.

As a result of the bulkiness of the ligand, as well as the additional aqua ligands on some the zinc atoms, the access to the pores is extremely limited; the opening to the pores is restricted to 3.5 × 3.5 Å.[102] This opening is too small to allow for the adsorption of methane, with a kinetic diameter of 3.76 Å, as predicted, yet was proposed to be useful in the separation of gases. The BET surface area was calculated to be 150 m^2/g with a pore volume of 0.10 cm^3/g; hydrogen uptake measurements at 77 K was measured to be 0.6 wt%.[102]

The stepwise growth from H_2ADC to 9,9'bianthryl-10,10'dicarboxylicacid (H_2BADC) is the next step in the growth of the linear, ditopic ligand series. H_2BADC was synthesized from a modified procedure (vide infra). The reaction between H_2BADC and $Zn(NO_3)_2 \cdot 6H_2O$ under solvothermal conditions produced block crystals PCN-81 which were characterized by X-ray diffraction (Table 3). PCN-81, a two-dimensional MOF, crystallizes in the space group C 2/c. In contrast to its three-dimensional block crystals, PCN-81 is a layered, non-porous framework as shown in Figure 23 and Figure 24. PCN-81 contains the zinc paddlewheel motif as its SBU with solvent molecules occupying the (Figure 25).

Table 3. Crystal data, data collection, and structure refinement for PCN-81.

Identification code	PCN-81
Empirical formula	$C_{68}H_{50}C_{l0}N_2O_{10}Zn_2$
Formula weight	1185.84
Temperature	110(2) K
Wavelength	0.71073 Å
Crystal system	Monoclinic
Space group	C 2/c
Unit cell dimensions	a = 21.759(2) Å, a= 90° b = 21.479(2) Å, b= 91.4280(10)° c = 11.3450(11) Å, g = 90°
Volume	5300.7(9) Å3
Z	4
Density (calculated)	1.486 Mg/m3
Absorption coefficient	0.973 mm-1
F(000)	2448
Crystal size	0.20 x 0.18 x 0.18 mm3
Theta range for data collection	1.87 to 28.33°
Index ranges	-28<=h<=28, -28<=k<=28, -15<=l<=15
Reflections collected	32471
Independent reflections	6601 [R(int) = 0.1030]
Completeness to theta = 28.33°	99.60%
Absorption correction	Semi-empirical from equivalents
Max. and min. transmission	0.8443 and 0.8291
Refinement method	Full-matrix least-squares on F2
Data / restraints / parameters	6601 / 5 / 373
Goodness-of-fit on F2	1.049
Final R indices [I>2sigma(I)]	R1 = 0.0621, wR2 = 0.1452
R indices (all data)	R1 = 0.1091, wR2 = 0.1662
Largest diff. peak and hole	1.791 and -1.547 e.Å-3

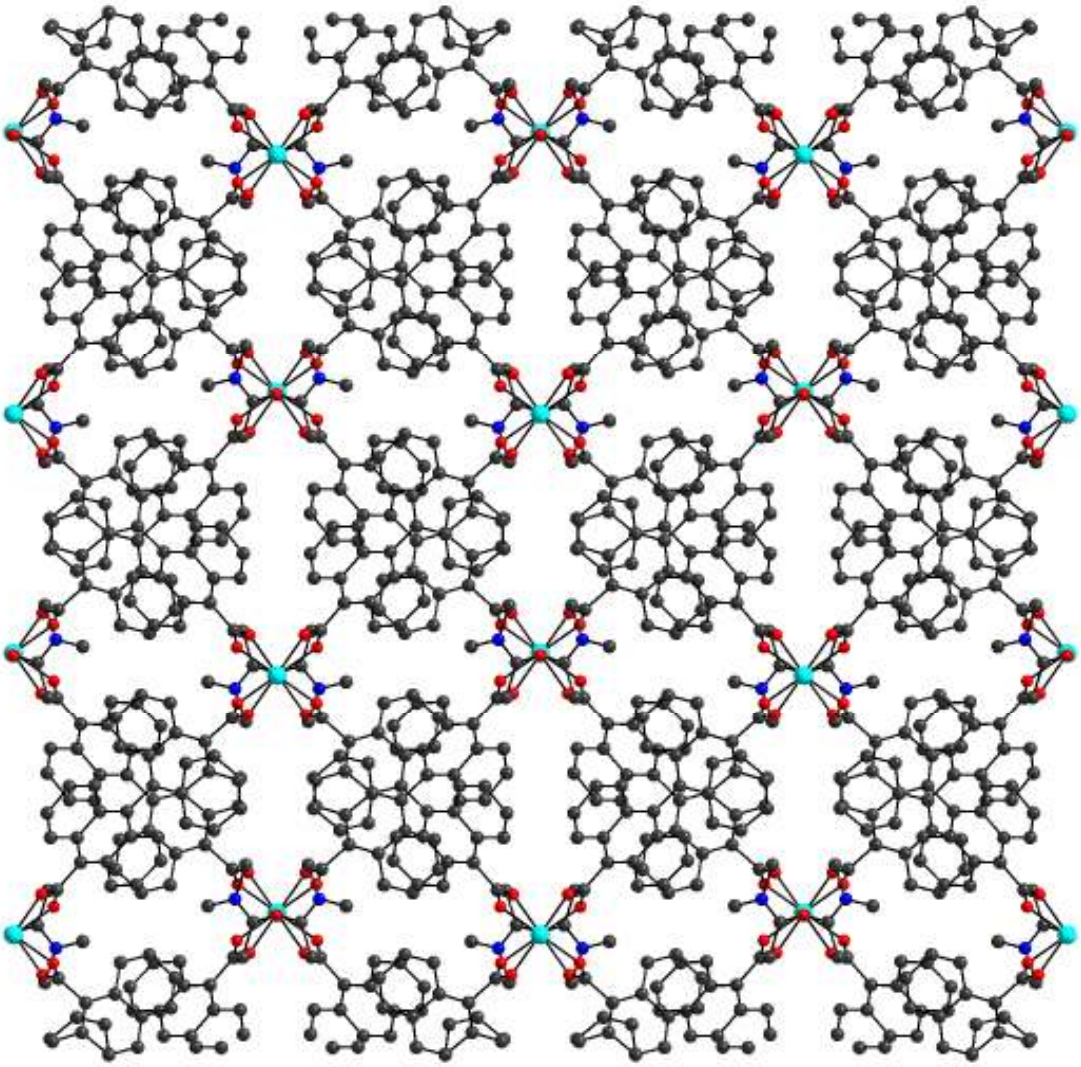

Figure 23. Extended framework of PCN-81 viewed down the [0,0,1] axis.

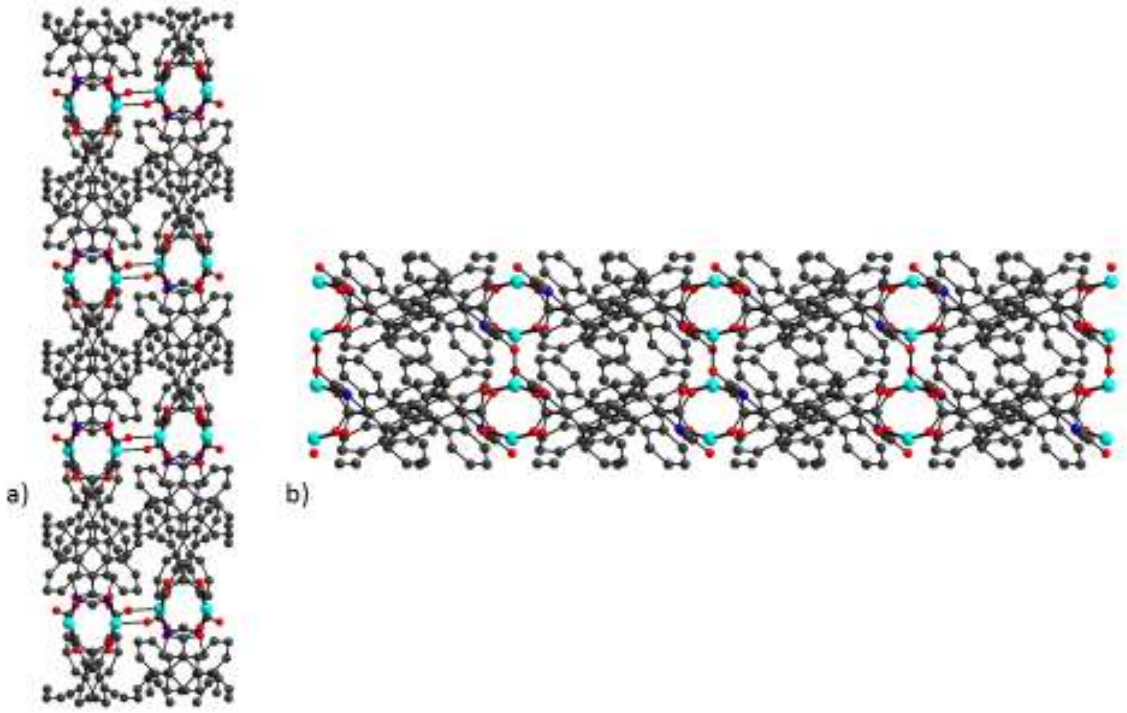

Figure 24. Views of PCN-81 from the a) [1,0,0} and b) [0,1,0] axes demonstrating the layered structure and lack of porosity.

Figure 25. Zn paddlewheel of PCN-81 with solvent molecules coordinated in the axial positions.

As with $BADBA^{2-}$, the $BADC^{2-}$ ligand deviates from the ideal 90° twist angle present in bianthryl as shown in Figure 26. The formation of a two-dimensional layered framework is unexpected considering the twist angle of approximately 90° that is present in $BADC^{2-}$. A two-dimensional framework is usually the result if paddlewheel SBUs are linked together with linear, planar, ditopic ligands.[103] However, for ligands that posses a 90° twist, a three-dimensional periodic network with the nbo topology is usually produced.[104] However, one must always be careful when assigning reticular properties to

solvothermal MOF reactions, as there are a multitude of factors which can influence the final structure.

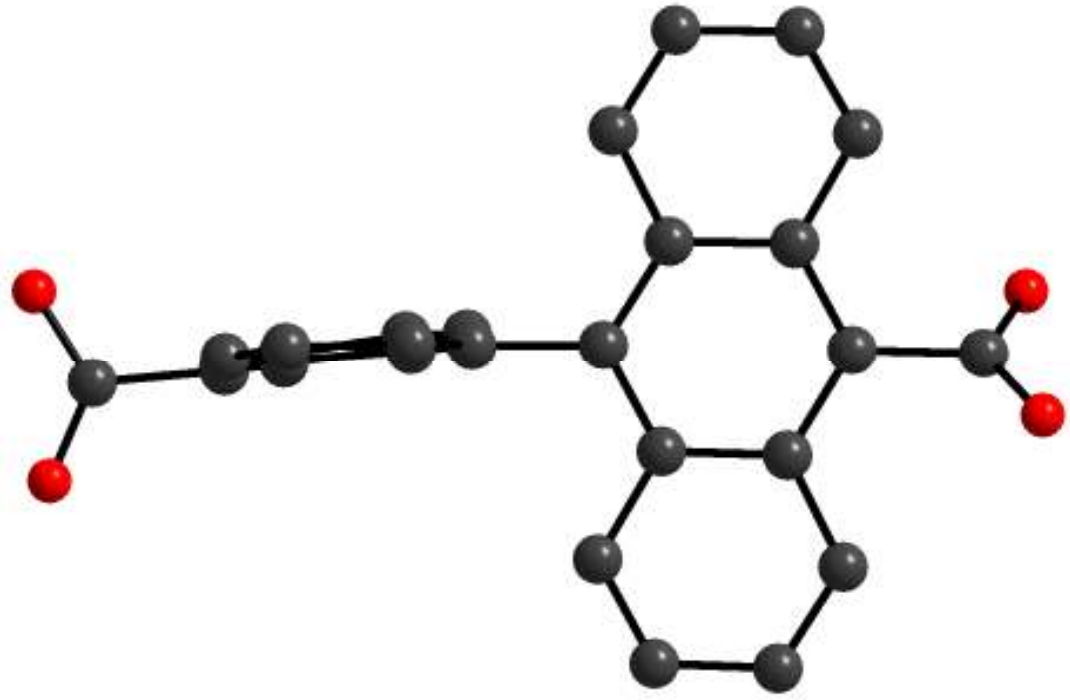

Figure 26. Structure of the ligand $BADC^{2-}$; the twist angle between the anthracene rings is 92.55°.

Molecular simulations were performed using Materials Studio 5.0. Figure 27 shows the simulated hydrogen adsorption isotherm which correlates to a maximum adsorption of 4.08 molecules of hydrogen per unit cell of PCN-81. The steep slope of the adsorption isotherm from 0 – 10 kPa is often present in frameworks with small pores. These small pores within the two-dimensional framework are responsible for the low hydrogen adsorption of 0.68 weight percent. However, the extremely high heat of adsorption of 12.19 kJ/mol indicates that what hydrogen is adsorbed interacts very strongly to the

framework. Evidence for the strong heat of adsorption is displayed in the steep rise in the adsorption isotherm of Figure 27. However, the flattening out at low pressures is indicative of the general lack of porosity present in PCN-81. Figure 28 shows the location of the simulated hydrogen adsorption.

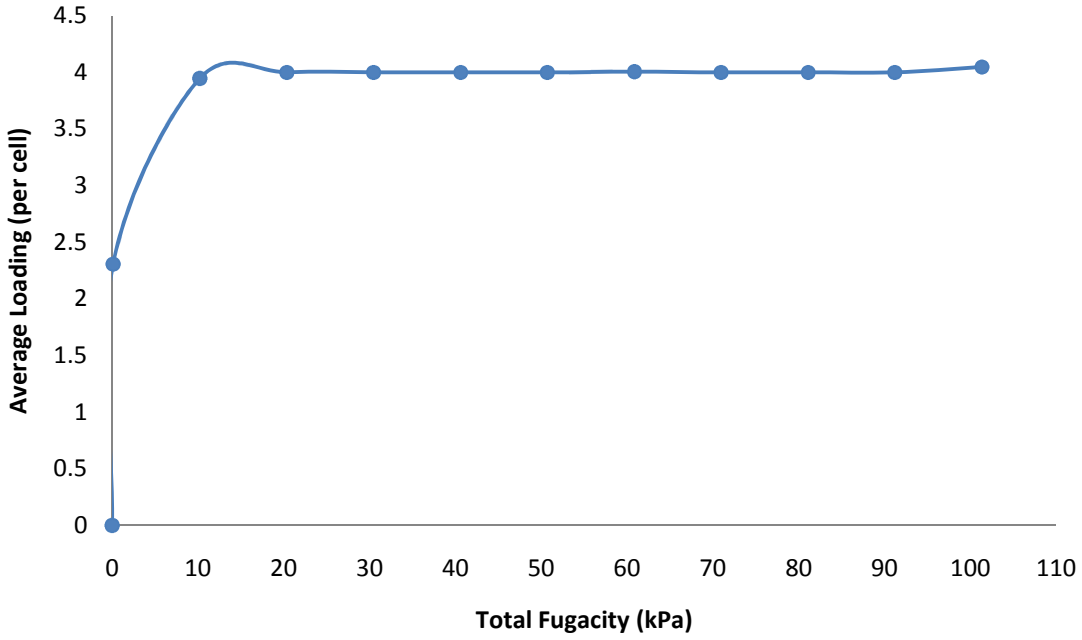

Figure 27. Simulated hydrogen adsorption isotherm for PCN-81 at 77 K.

a)

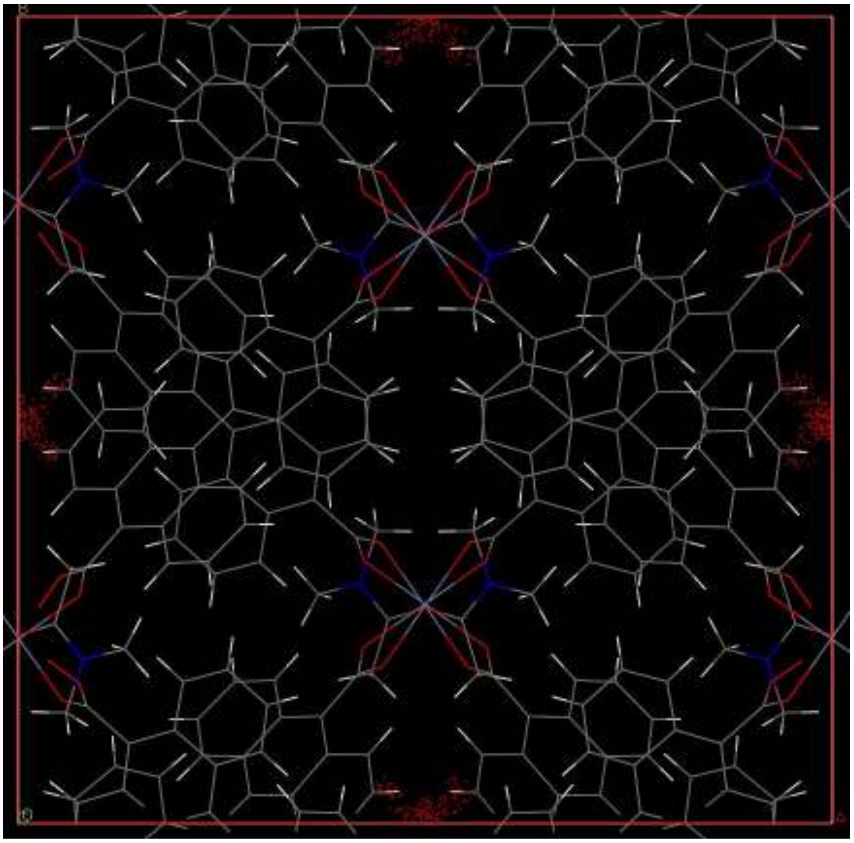

b)

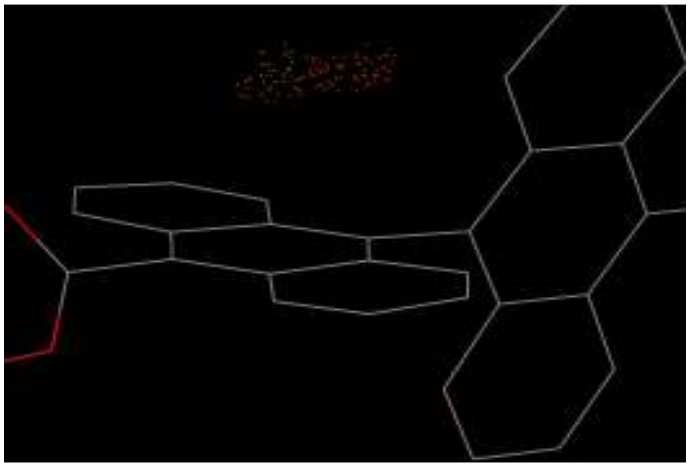

Figure 28. a) Simulated hydrogen adsorption in the unit cell of PCN-81; the red dots indicate the location of the adsorbed hydrogen and b) enlarged view of hydrogen adsorption above the anthracene rings (interwoven rings removed) with the scale of red to green of the hydrogen correlating to lower and higher bonding energies.

5.3 Comparison of frameworks

Table 4 highlights the data of the comparison. No distinct relationship was determined between the number of aromatic rings and any of the selected properties. With regard to hydrogen adsorption, it should be mentioned that improvements in gravimetric hydrogen uptake are often offset by the accompanying increase in density of the MOF.[105] Therefore, it is important to view the two properties not as individual entities but as functions of one another. If the increase in crystal density is a result of increasing the bulkiness of the ligand in an attempt to reduce the pore size, then the total hydrogen uptake will most likely increase.[16,106,107] However, in terms of adsorption by weight percent, this gain in adsorption will be offset by the overall increase in the molecular weight of the MOF. A balance between the two variables must be reached for an adsorbent to be utilized as a storage material for hydrogen.

Figure 29 visually illustrates the relationship between density and hydrogen adsorption for the study of the five chosen MOFs. PCN-80 is clearly the most attractive candidate for hydrogen adsorption as the hydrogen adsorbed by weight percent is nearly four times as great as that of MOF-5 while the crystal densities are fairly comparable. The other three MOFs have both extremely high crystal densities with very low hydrogen adsorption.

Table 4. Selected properties of stepwise increase in aromatic rings of MOFs' ligands. Hydrogen adsorption measurements taken under conditions of 77 K and 1 atm. * indicates lack of experimental data and therefore value was calculated from GCMC using Materials Studio 5.0. All data for PCN-80 and PCN-81 was calculated from GCMC simulations.

MOF	Ligand	Density (g/cm^3)	Surface Area (m^2/g)	Pore Volume (cm^3/g)	H_2 Uptake[a] (wt. %)	Ref.
MOF-5	BDC^{2-}	0.59	2885	1.18	1.15	60,108
MOF-48	NDC^{2-}	2.12*	710*	0.048*	0.44*	61
PCN-13	ADC^{2-}	1.24*	150	0.10	0.6	102
PCN-81	$BADC^{2-}$	1.49	156	0.0035	0.68	
PCN-80	$BADBA^{2-}$	0.66	3801	0.74	7.43	

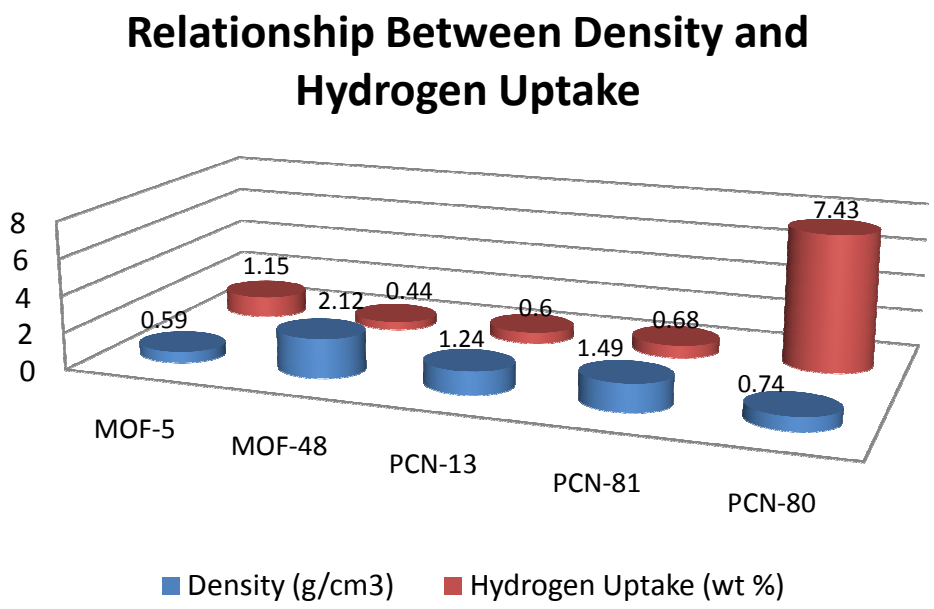

Figure 29. Comparison of framework densities with hydrogen adsorption at 77 K; a general trend exists in that the higher the crystal density, the lower the hydrogen uptake in weight percent.

The primary goal of this study was to generate a direct relationship between the number of aromatic rings in the ligand of the MOF and the adsorption of hydrogen. The weight percent of adsorbed hydrogen was used as that is perhaps most indicative measure of the usefulness of a MOF for a material in the application of on board vehicular hydrogen storage. Figure 30 visually depicts the results of the comparison studied. It is evident that no linear relationship exists. In fact, the generation of a fitted linear trend line to the data of Figure 30 results in an R^2 value of 0.451.

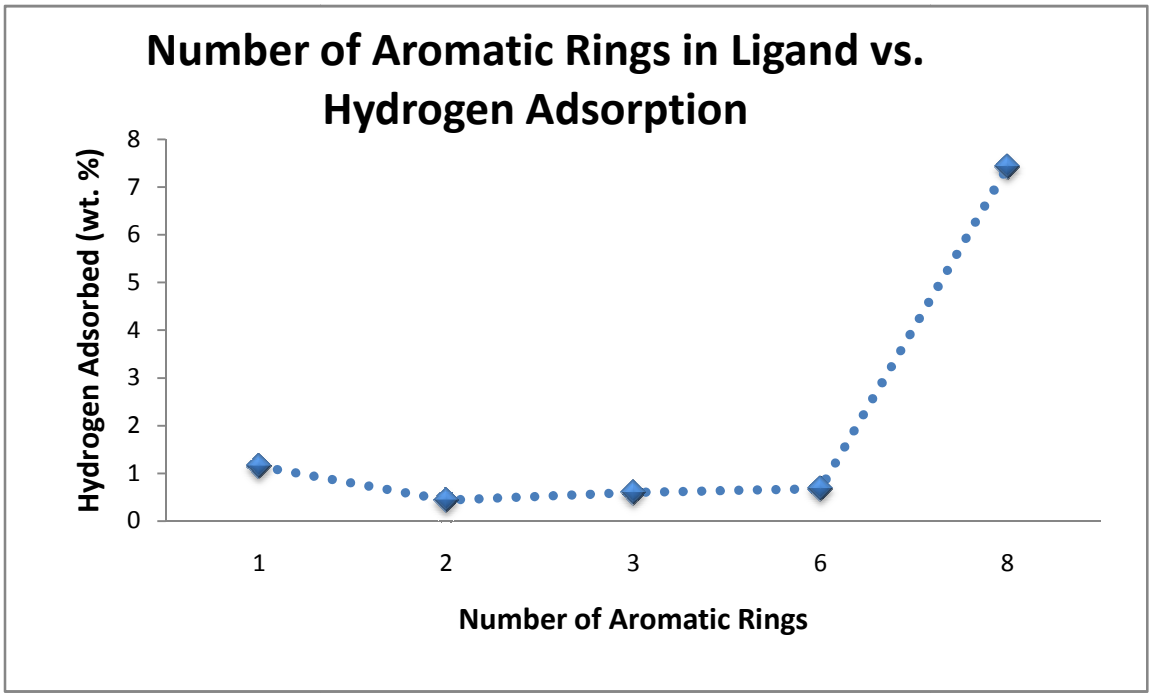

Figure 30. Relationship between aromatic rings in a ligand and weight percent of hydrogen adsorbed.

The lack of a clear relationship between the hydrogen uptake and aromatic rings can be explained by several deviations that were beyond the control of the experiment. For example, not all of the MOFs formed were three-dimensional; PCN-81 was a two-dimensional, non-porous layered structure. Additionally, the only three-dimensional interpenetrated framework was PCN-80, and it has been proven that interpenetration increases the hydrogen adsorption capacity (*vide supra*). Although all of the metal atoms in the SBU are Zn(II), the SBUs formed vary from Zn_4O to zinc paddlewheel to the combination of the two seen in PCN-80. This will have an impact on hydrogen uptake as open metal sites can adsorb more hydrogen than those that are occupied.

5.4 Future work

Along the c axis [0 0 1] the axial positions of the Zn paddlewheel are occupied by solvent molecules (Figure 25). The addition of a small, linear ditopic bridging ligand, such as 4,4'-bipyridine or pyrazine to name a few, to the solvothermal reaction may preferentially bind to the axial positions of the zinc atoms. If the binding atom is a nitrogen the chances of the bridging ligand binding to the metal instead of the solvent increases since the nitrogen atoms are more nucleophilic than oxygen atoms which will result in a better orbital overlap. The result of this would transform the 2D sheet of PCN-81 into a 3-D framework (which may or may not possess useful porosity)[5] by utilizing the bridging ligand to pillar the sheets. The choice of bridging ligand is crucial to the success of this potential extension. In order to ensure that the zinc paddlewheel unit is not altered, a neutral bridging ligand must be utilized. If an anionic ligand is employed in the reaction, the oxidation of the metal cluster will change to ensure charge balance. This could alter the SBU and the intended elongation along the [0 0 1] axis may not occur.

With the eight aromatic rings present in $BADBA^{2-}$ studies involving luminescence should be pursued. MOFs have been explored for their potential applications as luminescent materials with specific focus on fluorescent sensors and light emitting devices (LEDs)[109-112] Due to the chemical and thermal stability of MOFs, they have been suggested as superior replacements to organic molecules and polymers in regard to their luminescent properties.[109] The effects leading to such fluorescent behaviors include metal-centered luminescence, metal-to-ligand charge transfer, ligand-to-metal charge transfer, ligand-to-ligand charge transfer, ligand-centered luminescence, and metal-to-

metal charge transfer, metal-based emission, antennae effects, and adsorbate-based emission due to guest incorporation.[21] The study of MOFs being used for luminescent applications is in its infancy.

PCN-81, and PCN-80 for that matter, should be studied extensively for their luminescent properties. As a result of the bianthracene-based ligands that compose these MOFs displaying luminescent properties when dissolved in organic solvents such as dichloromethane (Figure 31), the luminescence of these MOFs is likely to be ligand based. Additionally, the metal ions of these MOFs should have a negligible influence on the electronic structure of the ligands as well as the cumulative effect of the interaction of multiple ligands as a result of the filled d-orbital of the Zn(II) metal ions.[21] More so, the increased conjugation of the ligands lowers the energy gap of the $\pi - \pi^*$ transition making the energy transfer to metal-based states much less desireable.[21] The adsorbance of guest molecules into the pores of PCN-80 or PCN-81, after the modifications necessary on the MOFs to create viable pores, may result in immobilization of the guest within close proximity to the source of luminescence which could lead to some interesting modification of the luminescence or new behavior altogether.[21] Much research needs to be done not only in the field of luminescent MOFs, but also in regards to the luminescent properties of PCN-80 and PCN-81.

Figure 31. Luminescence of H_2BADBA when exposed to UV lamp; pure compound dissolved in dichloromethane.

5.5 Synthesis

Synthesis of 9,9’-bianthracene-10,10’-dicarboxylic acid:

835 mg of 10,10’-dibromo-9,9'-bianthryl dissolved in 20 mL of dry diethyl ether and a stir bar were charged in a 50 mL Schlenk flask. The flask was filled with nitrogen and evacuated three times and then cooled to -78 °C with the aid of a dry ice – acetone bath. 2.7 mL of butyl lithium was added via a syringe causing the solution to turn from yellow to brownish-orange. The reaction was stirred at 20 minutes at -78 °C and then allowed to warm to room temperature where it was stirred for an additional 20 minutes. Dry ice was

placed in a large flask and a septum was attached. A needle attached to a bubbler filled with sulfuric acid through Tygon tubing was inserted into the septum. Tygon tubing was attached to the other end of the bubbler where a canula delivered the dry carbon dioxide gas into the reaction mixture. After five minutes of addition, the nitrogen was turned off and a vent needle allowed the excess carbon dioxide to escape. After 75 minutes, 10 mL of water was slowly added. A violent reaction occurred upon the addition of the water, so slow delivery was extremely important. 10 mL of diethyl ether was then added and the aqueous phase was washed with diethyl ether twice and acidified with 1 *M* sulfuric acid to yield 480 mg (66 % yield) of pure 9,9'-bianthracene-10,10'-dicarboxylic acid. ^{1}H NMR (DMSO-d_6): δ 14.0 (broad, OH), δ 8.19 (d, J = 8.7 Hz, 4 H), δ 7.61 (t, J = 6.9 Hz, 4 H), δ 7.27 (t, J = 8.7 Hz, 4 H), δ 6.92 (d, J = 8.7 Hz, 4 H). ^{13}C NMR (DMSO-d_6): δ 170.80, 134.03, 131.80, 130.65, 127.51, 127.24, 127.09, 126.63, 126.04.

Synthesis of PCN-81:

5.20 mg of H_2BADC and 7.00 mg of $Zn(NO_3)_2 \cdot 6H_2O$ were dissolved in a 0.5 dram vial with the aid of 1.5 mL of DMA and 3 drops of tetrafluroboric acid. The vial was placed in a 85 °C oven for 3 days until clear, block-like crystals of PCN-81 had formed.

CHAPTER VI

SUMMARY

6.1 Attempted synthesis of new metal-organic polyhedra

The first part of this thesis dealt with the creation of novel molecular polyhedra that not only should display unique properties but may, in the most idealistic sense, revolutionize the way MOFs are assembled by allowing for more control over the final framework topology (this revolution would be considered a small extension of the groundwork already laid by Li, Timmons, and Zhou's work[23]). Indeed, this work is in its infancy stage and the majority of Chapters II and III discussed the future possibilities and directions which the research should head.

Chapter II discussed the synthesis of a ligand precursor that would theoeretically synthesize a MOP that would neither fall into the Archimedean or Platonic types of MOPs. Although this precursor, 2,5 indole dicarboxylic acid, with a 150° bend-angle has been isolated and characterized, that is currently the extent of the progress of this project. Efforts have been made to synthesize such a crystal, yet to date no MOP crystals have been synthesized. Following the synthesis of the desired MOP, gas adsorption studies should be performed, as well as molecular inclusion experiments, to determine if the large cage is suitable for such applications. Following this, a new ligand precursor should be synthesized to form a cage in which the NH group of the indole points in towards the center of the cage. Subsequent experiments will determine whether or not the NH group has an effect of the selective adsorption of certain gases and molecules.

Going one step further would be to synthesize a MOP with a secondary amine and to test the polyhedron's ability to perform catalytic chemistry, specifically the Knoevenagel condensation.

Chapter III dealt with the attempted synthesis of a novel molecular polyhedron, which would then be extended into a framework based on the principles set forth by Li et al. The ligand precursor, 4,4'-(9-ethyl-9H-carbazole-3,6-diyl)dibenzoic acid, was synthesized and employed in several reaction schemes in an attempt to synthesize a MOP. Although no single crystals have been synthesized, efforts should continue to synthesize a crystal and elucidate its properties. As mentioned, the cage is expected to be bigger than that synthesized by Li et al.; should this be successfully synthesized and extended into a framework, the resulting MOF should possess openings in the MOP SBU greater than its predecessor. This MOF would be ideal for large molecule incorporation.

6.2 Synthesis of MOFs based on extended anthracene backbone

Chapters IV and V are somewhat related in the sense that the MOFs synthesized in both chapters stem from ligands containing a bianthracene backbone. PCN-80 is a triply-interpenetrated MOF containing a distorted Zn_4O SBU that, to the best of the author's knowledge, is the first of its kind. Normal Zn_4O SBUs, and even distorted ones, contain only zinc atoms that are only coordinated in a tetrahedral manner. One of the zinc atoms of the SBU in PCN-80 possesses an octahedral coordination environment. Efforts are underway to understand how and why this SBU was formed.

Due to the instability of PCN-80 in atmospheric conditions, gas adsorption experiments were unable to be performed. In lieu of these experiments, which are normally used to determine the surface area, pore volume, and gas uptake properties of a MOF, molecular simulations were carried out. These simulations revealed that PCN-80 has a surface area of 3801 m^2/g with a pore volume of 0.74 cm^3/g. Simulated isotherms for both hydrogen and methane uptake were also executed. PCN-80 exceeds, at least in theory, the DOE 2010 goal of 6 weight percent and 45 g/L, with a hydrogen adsorption of 7.43 weight percent and 61.47 g/L. A high pressure hydrogen adsorption isotherm was also simulated; this indicated that the adsorption capacity at 10000 kPa is 9.20 weight percent with a volumetric uptake of 75 g/L. Remarkably, this is greater than the density of hydrogen at 20.4 K. The strong isosteric heat of adsorption of 10.71 kJ/mol indicates a very strong interaction between the hydrogen and the framework. However, all of this data was derived from isotherms simulated at 77 K whereas the DOE targets are to be reached a minimum temperature of 243 K. Despite this shortcoming, PCN-80 possesses the highest hydrogen adsorption capacity at low pressure.

The ligand for PCN-80 was modeled after the anthracene-based ligand of PCN-14 in an attempt to exceed its methane adsorption capacity. The methane adsorption capacity was calculated to be 9.59 weight percent gravimetrically and 78.47 g/L (97.09 v/v). Although the maximum isosteric heat of adsorption 27.93 kJ/mol is among the highest reported for MOFs, the volumetric adsorption amounts to 44% of that of PCN-14 (220 v/v).[82] However, PCN-14's record breaking adsorption was at 35 bar whereas the simulation stops at 1 bar.

Although the original attempt of this project was to exceed the methane storage capacity of PCN-14, the structure of PCN-80 enables it to adsorb an unprecedented amount of hydrogen at low pressure and cryogenic temperatures. Indeed, these adsorption isotherms and capacities are simulations. Immediate work should be done to prepare a stable PCN-80 or synthesize a MOF with a similar structure so that experimental measurements can be obtained. On a structural level, research should be done to determine the reasons for the formation of the unique SBU. Further research will dictate whether the steric hindrance of the lengthy, bulky ligand or the synthetic conditions result in the novel SBU.

Chapter V attempted to elucidate a clear relationship between the hydrogen adsorption capacity of a framework and the number of aromatic rings used in the ligand. Five ligands were chosen, along with the resultant frameworks from their reaction with zinc metal salts. The numbers of aromatic rings used in the study were one, two, three, six, and eight. A linear, ditopic geometry was maintained throughout the experiment. MOF-5, MOF-48, PCN-13, PCN-81, and PCN-80 were the MOFs that were compared. For the MOFs that were synthesized by other authors that didn't have published data regarding surface area, pore volume, and hydrogen adsorption, simulations were performed using Materials Studio 5.0. The two dimensional PCN-81 was synthesized and simulations were performed to determine its properties. Adsorption isotherms indicated a maximum hydrogen uptake of 0.68 weight percent.

While no clear relationship was established between the number of aromatic rings and the maximum adsorption capacity for the MOF, a pattern was confirmed regarding

density and hydrogen adsorption capacity: generally speaking the lower the density, the greater the hydrogen adsorption capacity. However, a variety of factors may have influenced these results. For example, not all of the MOFs contain identical SBUs: some possess the Zn_4O SBU while others have the zinc paddlewheel. Likewise, PCN-80 was the only MOF with three-fold interpenetration and PCN-81 was the only two-dimensional MOF.

Future work should first and foremost focus on changing PCN-81 from a two-dimensional to a three-dimensional MOF. A neutral, ditopic linker such as 4,4'-bipyradine should be added to the reaction to form PCN-81 in hopes that the axially coordinated solvent of the zinc paddlewheel is displaced by the bipyridine to form an extended, three dimensional framework. This should increase the pore volume, and thus the adsorption capacity for hydrogen.

6.3 Conclusion

The research presented in this thesis primarily focuses on the two main aspects of MOP and MOF research: ligand design and characterization. The synthesis of novel ligands is essential to the advancement of the field as synthetic schemes with purchasable ligands have all but been exhausted. Chapters III, IV, and V contain the synthesis of, to the best of the author's knowledge, novel ligands. Consequently, PCN-80 and PCN-81 are the first examples of frameworks formed from a ligand with a bianthracene backbone. The unprecedented hydrogen adsorption of PCN-80 at low pressure is indeed exciting, yet this preliminary calculation needs to be verified with

hard, experimental data; this task should be pursued with a sense of urgency. Additionally, methane uptake experiments should be performed to see if PCN-80 is a suitable candidate for methane storage. The addition of a neutral, linear, ditopic linker to the reaction scheme between H_2BADC and zinc nitrate should yield a three-dimensional MOF. Such a MOF might aid in the study of the effect of additional aromatic rings on hydrogen uptake.

Most of the work presented in this thesis contains little more than preliminary results. The groundwork has been laid, and interested researchers should pick up where this research left off. Monumental breakthroughs in terms of large MOPs and hydrogen and methane storage in MOFs potentially lie in this thesis.

REFERENCES

(1) Kuppler, R. J.; Timmons, D. J.; Fang, Q.-R.; Li, J.-R.; Makal, T. A.; Young, M. D.; Yuan, D.; Zhao, D.; Zhuang, W.; Zhou, H.-C. *Coordination Chemistry Reviews* **2009**, *253*, 3042-3066.

(2) Rouquerol, J.; Avnir, D.; Fairbridge, C. W.; Everett, D. H.; Haynes, J. H.; Pernicone, N.; Ramsay, J. D. F.; Sing, K. S. W.; Unger, K. K. *Pure and Applied Cheistry* **1994**, *66*, 1739-58.

(3) Brunauer, S.; Deming, L. S.; Deming, W. E.; Teller, E. *Journal of the American Chemical Society* **1940**, *62*, 1723-1732.

(4) Gregg, S. J.; Sing, K. S. W. *Adsorption, Surface Area and Porosity. 2nd Ed*; Academic Press: London **1982**.

(5) Kitagawa, S.; Kitaura, R.; Noro, S. *Angewandte Chemie-International Edition* **2004**, *43*, 2334-2375.

(6) Manocha, S. M. *Sadhana* **2003**, *28*, 335-348.

(7) Marsh, H. *Activated Carbon*; Elsevier: Amsterdam, **2006**.

(8) Breck, D. W. *Zeolite Molecular Sieves: Structure, Chemistry, and Use*; John Wiley & Sons: New York, **1974**.

(9) Ferey, G. *Chemistry of Materials* **2001**, *13*, 3084-3098.

(10) Férey, G. *Chemical Society Reviews* **2008**, *37*, 191-214.

(11) Davis, M. E.; Lobo, R. F. *Chemistry of Materials* **1992**, *4*, 756-768.

(12) Rowsell, J. L. C.; Yaghi, O. M. *Microporous and Mesoporous Materials* **2004**, *73*, 3-14.

(13) Tranchemontagne, David J.; Ni, Z.; O'Keeffe, M.; Yaghi, Omar M. *Angewandte Chemie International Edition* **2008**, *47*, 5136-5147.

(14) Park, Young K.; Choi, Sang B.; Kim, H.; Kim, K.; Won, B.-H.; Choi, K.; Choi, J.-S.; Ahn, W.-S.; Won, N.; Kim, S.; Jung, Dong H.; Choi, S.-H.; Kim, G.-H.; Cha, S.-S.; Jhon, Young H.; Yang, Jin K.; Kim, J. *Angewandte Chemie International Edition* **2007**, *46*, 8230-8233.

(15) Morris, R. E.; Wheatley, P. S. *Angewandte Chemie-International Edition* **2008**, *47*, 4966-4981.

(16) Zhao, D.; Yuan, D. Q.; Zhou, H. C. *Energy & Environmental Science* **2008**, *1*, 222-235.

(17) Murray, L. J.; Dinca, M.; Long, J. R. *Chemical Society Reviews* **2009**, *38*, 1294-1314.

(18) Li, J.-R.; Kuppler, R. J.; Zhou, H. C. *Chemical Society Reviews* **2009**, *38*, 1477-1504.

(19) Kitagawa, S.; Uemura, K. *Chemical Society Reviews* **2005**, *34*, 109-119.

(20) Lee, J.; Farha, O. K.; Roberts, J.; Scheidt, K. A.; Nguyen, S. T.; Hupp, J. T. *Chemical Society Reviews* **2009**, *38*, 1450-1459.

(21) Allendorf, M. D.; Bauer, C. A.; Bhakta, R. K.; Houk, R. J. T. *Chemical Society Reviews* **2009**, *38*, 1330-1352.

(22) Vallet-Regí, M.; Balas, F.; Arcos, D. *Angewandte Chemie International Edition* **2007**, *46*, 7548-7558.

(23) Li, J.-R.; Timmons, D. J.; Zhou, H.-C. *Journal of the American Chemical Society* **2009**, *131*, 6368-6369.

(24) Hoskins, B. F.; Robson, R. *Journal of the American Chemical Society* **1990**, *112*, 1546-54.

(25) Ma, S. Q.; Eckert, J.; Forster, P. M.; Yoon, J. W.; Hwang, Y. K.; Chang, J. S.; Collier, C. D.; Parise, J. B.; Zhou, H. C. *Journal of the American Chemical Society* **2008**, *130*, 15896-15902.

(26) Tranchemontagne, D. J.; Mendoza-Cotres, J. L.; O'Keeffe, M.; Yaghi, O. M. *Chemical Society Reviews* **2009**, *38*, 1257-1283.

(27) Eddaoudi, M.; Moler, D. B.; Li, H.; Chen, B.; Reineke, T. M.; O'Keeffe, M.; Yaghi, O. M. *Accounts of Chemical Research* **2001**, *34*, 319-330.

(28) O'Keeffe, M.; Eddaoudi, M.; Li, H.; Reineke, T.; Yaghi, O. M. *Journal of Solid State Chemistry* **2000**, *152*, 3-20.

(29) Batten, S. R.; Neville, S. M.; Turner, D. R. *Coordination Polymers: Design, Analysis and Application*; Royal Society of Chemistry: Cambridge, 2009.

(30) O'Keeffe, M.; Eddaoudi, M.; Li, H. L.; Reineke, T.; Yaghi, O. M. *Journal of Solid State Chemistry* **2000**, *152*, 3-20.

(31) Kurmoo, M. *Chemical Society Reviews* **2009**, *38*, 1353-1379.

(32) Banerjee, R.; Phan, A.; Wang, B.; Knobler, C.; Furukawa, H.; O'Keeffe, M.; Yaghi, O. M. *Science* **2008**, *319*, 939-943.

(33) Biemmi, E.; Christian, S.; Stock, N.; Bein, T. *Microporous and Mesoporous Materials* **2008**, *117*, 111-117.

(34) Tompsett, G. A.; Conner, W. C.; Yngvesson, K. S. *ChemPhysChem* **2006**, *7*, 296-319.

(35) Bae, Y.-S.; Mulfort, K. L.; Frost, H.; Ryan, P.; Punnathanam, S.; Broadbelt, L. J.; Hupp, J. T.; Snurr, R. Q. *Langmuir* **2008**, *24*, 8592-8598.

(36) Jhung, S. H.; Yoon, J. W.; Hwang, J.-S.; Cheetham, A. K.; Chang, J.-S. *Chemistry of Materials* **2005**, *17*, 4455-4460.

(37) Collins, C. S.; Sun, D.; Liu, W.; Zuo, J.-L.; Zhou, H.-C. *Journal of Molecular Structure* **2008**, *890*, 163-169.

(38) Sudik, A. C.; Millward, A. R.; Ockwig, N. W.; Cote, A. P.; Kim, J.; Yaghi, O. M. *Journal of the American Chemical Society* **2005**, *127*, 7110-7118.

(39) Fujita, M. *Chemical Society Reviews* **1998**, *27*, 417-425.

(40) David J. Tranchemontagne, Z. N., Michael O'Keeffe, Omar M. Yaghi, *Angewandte Chemie International Edition* **2008**, *47*, 5136-5147.

(41) Ke, Y. X.; Collins, D. J.; Zhou, H. C. *Inorganic Chemistry* **2005**, *44*, 4154-4156.

(42) Moulton, B.; Lu, J. J.; Mondal, A.; Zaworotko, M. J. *Chemical Communications* **2001**, 863-864.

(43) Furukawa, H.; Kim, J.; Ockwig, N. W.; O'Keeffe, M.; Yaghi, O. M. *Journal of the American Chemical Society* **2008**, *130*, 11650-11661.

(44) Eddaoudi, M.; Kim, J.; Wachter, J. B.; Chae, H. K.; O'Keeffe, M.; Yaghi, O. M. *Journal of the American Chemical Society* **2001**, *123*, 4368-4369.

(45) Park, J.; Hong, S.; Moon, D.; Park, M.; Lee, K.; Kang, S.; Zou, Y.; John, R. P.; Kim, G. H.; Lah, M. S. *Inorganic Chemistry* **2007**, *46*, 10208-10213.

(46) Zou, Y.; Park, M.; Hong, S.; Lah, M. S. *Chemical Communications* **2008**, 2340-2342.

(47) Prakash, M. J.; Zou, Y.; Hong, S.; Park, M.; Bui, M.-P. N.; Seong, G. H.; Lah, M. S. *Inorganic Chemistry* **2009**, *48*, 1281-1283.

(48) Wang, Y.; Cheng, P.; Song, Y.; Liao, D. Z.; Yanl, S. P. *Chemistry - A European Journal* **2007**, *13*, 8131-8138.

(49) Sudik, A. C.; Millward, A. R.; Ockwig, N. W.; Cote, A. P.; Kim, J.; Yaghi, O. M. *Journal of the American Chemical Society* **2005**, *127*, 7110-7118.

(50) Hamilton, T. D.; Papaefstathiou, G. S.; FrisÌŒcÌŒicÌ , T.; BucÌŒar, D.-K.; MacGillivray, L. R. *Journal of the American Chemical Society* **2008**, *130*, 14366-14367.

(51) Seo, J. S.; Whang, D.; Lee, H.; Jun, S. I.; Oh, J.; Jeon, Y. J.; Kim, K. *Nature* **2000**, *404*, 982-986.

(52) Khalaf, A. I.; Pitt, A. R.; Scobie, M.; Suckling, C. J.; Urwin, J.; Waigh, R. D.; Fishleigh, R. V.; Young, S. C. *J. Chem. Res., Synop.* **2000**, 264-265.

(53) Lindwall, H. G.; Mantell, G. J. *The Journal of Organic Chemistry* **1953**, *18*, 345-357.

(54) Utting, K. A.; Macquarrie, D. J. *Appl. Catal., A* **2002**, *232*, 7-12.

(55) Fioravanti, S.; Pellacani, L.; Tardella, P. A.; Vergari, M. C. *Organic Letters* **2008**, *10*, 1449-1451.

(56) Perry; Kravtsov, V. C.; McManus, G. J.; Zaworotko, M. J. *Journal of the American Chemical Society* **2007**, *129*, 10076-10077.

(57) Sudik, A. C.; Côté, A. P.; Wong-Foy, A. G.; O'Keeffe, M.; Yaghi, O. M. *Angewandte Chemie International Edition* **2006**, *45*, 2528-2533.

(58) Jansen, M.; Schön, J. C. *Angewandte Chemie International Edition* **2006**, *45*, 3406-3412.

(59) Chun, H. *Journal of the American Chemical Society* **2008**, *130*, 800-801.

(60) Li, H.; Eddaoudi, M.; O'Keeffe, M.; Yaghi, O. M. *Nature* **1999**, *402*, 276-279.

(61) Eddaoudi, M.; Kim, J.; Rosi, N.; Vodak, D.; Wachter, J.; O'Keeffe, M.; Yaghi, O. M. *Science* **2002**, *295*, 469-472.

(62) Chen, B. L.; Ma, S. Q.; Hurtado, E. J.; Lobkovsky, E. B.; Zhou, H. C. *Inorganic Chemistry* **2007**, *46*, 8490-8492.

(63) Perry, J. J.; Perman, J. A.; Zaworotko, M. J. *Chemical Society Reviews* **2009**, *38*, 1400-1417.

(64) van den Berg, A. W. C.; Areán, C. O. *Chemical Communications* **2008**, 668-681.

(65) Schlapbach, L.; Züttel, A. *Nature* **2001**, *414*, 353-358.

(66) Wang, L. F.; Yang, R. T. *Energy & Environmental Science* **2008**, *1*, 268-279.

(67) Murray, L. J.; Dincă, M.; Long, J. R. *Chemical Society Reviews* **2009**, *38*, 1294-1314.

(68) Grochala, W.; Edwards, P. P. *Chemical Reviews* **2004**, *104*, 1283-1316.

(69) Mandal, T. K.; Gregory, D. H. *Annual Reports Section "A" (Inorganic Chemistry)* **2009**, *105*, 21-54.

(70) Collins, D. J.; Zhou, H. C. *Journal of Materials Chemistry* **2007**, *17*, 3154-3160.

(71) Ma, S. Q. *Pure and Applied Chemistry* **2009**, *81*, 2235-2251.

(72) Rowsell, J. L. C.; Yaghi, O. M. *Angewandte Chemie-International Edition* **2005**, *44*, 4670-4679.

(73) Lin, X.; Jia, J.; Zhao, X.; Thomas, K. M.; Blake, A. J.; Walker, G. S.; Champness, N. R.; Hubberstey, P.; Schröder, M. *Angewandte Chemie International Edition* **2006**, *45*, 7358-7364.

(74) Sagara, T.; Klassen, J.; Ortony, J.; Ganz, E. *Journal of Chemical Physics* **2005**, *123*.

(75) International Panel on Climate Change, Carbon Dioxide Capture and Storage; Cambridge University Press: New York **2005**.

(76) Menon, V. C.; Komarneni, S. *Journal of Porous Materials* **1998**, *5*, 43-58.

(77) Düren, T.; Sarkisov, L.; Yaghi, O. M.; Snurr, R. Q. *Langmuir* **2004**, *20*, 2683-2689.

(78) Cracknell, R. F.; Gordon, P.; Gubbins, K. E. *The Journal of Physical Chemistry* **1993**, *97*, 494-499.

(79) Ruthven, D. M. *Principles of Adsorption and Adsorption Processes* John Wiley& Sons: New York, **1984**.

(80) Duren, T.; Snurr, R. Q. *Journal of Physical Chemistry B* **2004**, *108*, 15703-15708.

(81) Wu, H.; Simmons, Jason M.; Liu, Y.; Brown, Craig M.; Wang, X.-S.; Ma, S.; Peterson, Vanessa K.; Southon, Peter D.; Kepert, Cameron J.; Zhou, H.-C.; Yildirim, T.; Zhou, W. *Chemistry - A European Journal* **2010**, *16*, 5205-5214.

(82) Ma, S. Q.; Sun, D. F.; Simmons, J. M.; Collier, C. D.; Yuan, D. Q.; Zhou, H. C. *Journal of the American Chemical Society* **2008**, *130*, 1012-1016.

(83) Wu, H.; Simmons, Jason M.; Liu, Y.; Brown, Craig M.; Wang, X.-S.; Ma, S.; Peterson, Vanessa K.; Southon, Peter D.; Kepert, Cameron J.; Zhou, H.-C.; Yildirim, T.; Zhou, W. *Chemistry - A European Journal*, *9999*, **2010**.

(84) Wu, H.; Zhou, W.; Yildirim, T. *Journal of the American Chemical Society* **2009**, *131*, 4995-5000.

(85) Yang, Q.; Zhong, C. *Journal of Physical Chemistry B* **2006**, *110*, 17776-17783.

(86) Dueren, T.; Bae, Y.-S.; Snurr, R. Q. *Chemical Society Reviews* **2009**, *38*, 1237-1247.

(87) Keskin, S.; Liu, J.; Rankin, R. B.; Johnson, J. K.; Sholl, D. S. *Industrial & Engineering Chemistry Research* **2009**, *48*, 2355-2371.

(88) Dueren, T.; Millange, F.; Ferey, G.; Walton, K. S.; Snurr, R. Q. *Journal of Physical Chemistry C* **2007**, *111*, 15350-15356.

(89) Brunauer, S.; Emmett, P. H.; Teller, E. *Journal of the American Chemical Society* **1938**, *60*, 309-319.

(90) Kyziol, J. B.; Zaleski, J. *Acta Crystallographica Section E* **2007**, *63*, o1235-o1237.

(91) Kaye, S. S.; Dailly, A.; Yaghi, O. M.; Long, J. R. *Journal of the American Chemical Society* **2007**, *129*, 14176-14177.

(92) Sun, D.; Ma, S.; Ke, Y.; Collins, D. J.; Zhou, H.-C. *Journal of the American Chemical Society* **2006**, *128*, 3896-3897.

(93) Ma, S.; Zhou, H.-C. *Journal of the American Chemical Society* **2006**, *128*, 11734-5.

(94) Duren, T.; Sarkisov, L.; Yaghi, O. M.; Snurr, R. Q. *Langmuir* **2004**, *20*, 2683-2689.

(95) Panella, B.; Hirscher, M.; Pütter, H.; Müller, U. *Advanced Functional Materials* **2006**, *16*, 520-524.

(96) Rosi, N. L.; Eckert, J.; Eddaoudi, M.; Vodak, D. T.; Kim, J.; O'Keeffe, M.; Yaghi, O. M. *Science* **2003**, *300*, 1127-1129.

(97) Ooms, K. J.; Wasylishen, R. E. *Microporous and Mesoporous Materials* **2007**, *103*, 341-351.

(98) Wong-Foy, A. G.; Matzger, A. J.; Yaghi, O. M. *Journal of the American Chemical Society* **2006**, *128*, 3494-3495.

(99) Panella, B.; Hirscher, M. *Advanced Materials* **2005**, *17*, 538-541.

(100) Rowsell, J. L. C.; Millward, A. R.; Park, K. S.; Yaghi, O. M. *Journal of the American Chemical Society* **2004**, *126*, 5666-5667.

(101) Vodak, D. T.; Braun, M. E.; Kim, J.; Eddaoudi, M.; Yaghi, O. M. *Chemical Communications* **2001**, 2534-2535.

(102) Ma, S.; Wang, X.-S.; Collier, C. D.; Manis, E. S.; Zhou, H.-C. *Inorganic Chemistry* **2007**, *46*, 8499-8501.

(103) Hawxwell, S. M.; Adams, H.; Brammer, L. *Acta Crystallographica Section B* **2006**, *62*, 808-814.

(104) Furukawa, H.; Kim, J.; Ockwig, N. W.; Oâ€™Keeffe, M.; Yaghi, O. M. *Journal of the American Chemical Society* **2008**, *130*, 11650-11661.

(105) Rowsell, J. L. C.; Yaghi, O. M. *Angewandte Chemie International Edition* **2005**, *44*, 4670-4679.

(106) Yang, C.; Wang, X.; Omary, M. A. *Journal of the American Chemical Society* **2007**, *129*, 15454-15455.

(107) Pan, L.; Sander, M. B.; Huang, X.; Li, J.; Smith, M.; Bittner, E.; Bockrath, B.; Johnson, J. K. *Journal of the American Chemical Society* **2004**, *126*, 1308-1309.

(108) Sabo, M.; Henschel, A.; Froede, H.; Klemm, E.; Kaskel, S. *Journal of Materials Chemistry* **2007**, *17*, 3827-3832.

(109) Huh, S.; Jung, S.; Kim, Y.; Kim, S.-J.; Park, S. *Dalton Transactions* **2010**, *39*, 1261-1265.

(110) Kraft, A.; Grimsdale, A. C.; Holmes, A. B. *Angewandte Chemie International Edition* **1998**, *37*, 402-428.

(111) Janiak, C. *Dalton Transactions* **2003**, 2781-2804.

(112) Suh, M. P.; Cheon, Y. E.; Lee, E. Y. *Coordination Chemistry Reviews* **2008**, *252*, 1007-1026.

VITA

Ryan John Kuppler received his Bachelor of Arts in chemistry from Miami University in Oxford, Ohio in 2008. That summer he joined Professor Hong-Cai Zhou's research lab at Texas A&M University. His research focused on creating new porous materials for applications in alternative energy solutions such as gas storage, selective gas adsorption, and possibly catalysis. He graduated with his Master of Science in August 2010.

A chemist by training, an avid home brewer by birth, Ryan enjoys brewing craft beers for his wife and himself. Additionally, he is an amateur triathlete and an accomplished conversationalist. Evenings and weekends are occupied by family walks and trips to the dog park with the loveable dog, McCoy. Ryan plans on using his science training to further his brewing hobby and one day open a microbrewery. Until then, he will begin his career as a high school chemistry teacher in Bryan, Texas; an altruistic goal that is most likely a result of his career being cut short (a-la Bo Jackson-style) preventing him from becoming a professor.

Ryan can be reached via his professor at Dept. of Chemistry, Texas A&M University, PO Box 30012, College Station, TX 77842-3012 care of Hong-Cai Zhou. His email is Kuppler.Ryan@gmail.com and he welcomes all comments and salutations.